D2.8

Report on Geomechanical results for the 3 areas

Release Status: Final

Authors: Marc Fleury, Axelle Baroni, João Barradas, Paula Canteli, Julio Carneiro, João Casacão, Paula Faria, Johann Fernandes, Elena Fernandez de Arévalo, Jesús García Crespo, David García F.-Valderrama, Nikolaos Koukouzas, Daniel Marques da Silva, Javier Martinez, Jose Mediato, Patricia Moita, Francisco Pangaro Bedoya, Jorge Pedro, Bruno Pina, Carlos Ribeiro, Nicolas Rousseau, Pavlos Tyrologou, Mark Wilkinson

Date: 27 February 2023

Filename and Version: D2.8_PilotSTRATEGY_Geomechanics

PilotSTRATEGY (H2020- Topic LC-SC3-NZE-6-2020 - RIA)

1. Document History

1.1 Location

This document is stored in the following location:

Filename	D2.8_PilotSTRATEGY_Geomechanics
Location	https://pilotstrategy.eu/about-the-project/work-packages/geo-characterisation

1.2 Revision History

This document has been through the following revisions:

Version No.	Revision Date	Filename/Location stored:	Brief Summary of Changes
1.0	27 Feb 2023		
1.1	07 March 2023		Request figure with lithological schematic section with samples and pictures placed

1.3 Authorisation

This document requires the following approvals:

AUTHORISATION	Name	Signature	Date
WP Leader	M. Wilkinson,		04/04/2023
Project Coordinator	Fernanda de Mesquita Lobo Veloso		04/04/2023

1.4 Distribution

This document has been distributed to:

Name	Title	Version Issued	Date of Issue
		PUBLIC	00/00/0000

The PilotSTRATEGY project has received funding from the European Union's Horizon 2020 research and innovation programme under grant agreement No. 101022664

Disclaimer

The information and views set out in this report are those of the author(s) and do not necessarily reflect the official opinion of the European Union. Neither the European Union institutions and bodies nor any person acting on their behalf may be held responsible for the use which may be made of the information contained therein.

The PilotSTRATEGY project has received funding from the European Union's Horizon 2020 research and innovation programme under grant agreement No. 101022664

2. Executive summary

This deliverable reports on the geomechanical data collected for all sites in France, Spain (off-shore and on-shore), Portugal and Greece. The source of information and sample gathering can be extremely variable: for France and Spain (on-shore), well samples were available from the oil exploration period; in Spain off-shore and Portugal, well log data were used essentially together with a few samples; in Greece, outcrop samples were used. For each region, a brief geological description is made to describe the formation target and the general context.

The purpose of the geomechanical data is to provide the parameters of the geomechanical model. An accurate estimation of elastic properties in reservoir layers is required in order to predict induced stress and strain variations due to changes in pressure, while the plastic properties are required for risk assessment as it defines the elastic limit of the formation beyond which deformations become irreversible. The data acquired give a partial view of the properties of the sites, and one of the challenges of the modelling will be to distribute the properties throughout the model.

For the Paris Basin (France), the measurement results are limited in number because there were few samples and because of very rigorous sample requirements. Elastic properties of the samples from the Charmottes well samples follow the carbonate geomechanical model of IFPEN, while the Vulaines samples have weaker mechanical properties for the measured porosity.

For the onshore Ebro Basin (Spain), a complete geomechanical characterization was carried out on the Torre de las Arcas section where good quality drilled samples were available, with additional field measurements on samples too soft to core. Significant differences in the mechanical response of rocks were found comparing materials of different sedimentary facies.

For the offshore Ebro basin, core samples suitable for analysis were not available. To overcome this, rock properties have been calculated using data from well logs using standard geophysical relationships for 3 wells. This work has obtained elastic parameters that are the best approximation with the data available to populate any future dynamic model in the area.

For the Lusitania Basin (Portugal), samples were taken from outcrops, the lack of samples collected at depths equivalent to the required depth for carbon storage is a constraint for the interpretation of the results. Laboratory measurement of the Point Load Strength Index Test was conducted with the determination of Uniaxial Compressive Strength using a Schmidt Hammer.

For the West Macedonia area (Greece), representative samples were collected at outcrops and tested for the required parameters. As with the Portugal samples, there is the question of how representative these are of the subsurface.

The PilotSTRATEGY project has received funding from the European Union's Horizon 2020 research and innovation programme under grant agreement No. 101022664

Table of Contents

The PilotSTRATEGY project has received funding from the European Union's Horizon 2020 research and innovation programme under grant agreement No. 101022664

The PilotSTRATEGY project has received funding from the European Union's Horizon 2020 research and innovation programme under grant agreement No. 101022664

3. Samples from France

3.1 Geological aspects

3.1.1 Geological settings of the area of interest

The French study area is located in the Paris Basin, some 60 Km Southwest to Paris (Fig. 1a), next to the Nangis locality. This area has been a preferential target for oil exploration at the second half of the 20th century, as shown in Figure 1b with the numbers of the wells used in our study. Nowadays a high volume of wells, well logs, and cores data are in the public domain and used in this study to understand the "Oolithe Blanche" Formation, the target reservoir in the French Area for the PilotSTRATEGY Project (Fig 1c). Thanks to this important array of data, the French team were able to conduct an import works of thin section analyses, core description (477m) through 12 wells (Fig. 1b) and well correlation in the area (51 wells correlated).

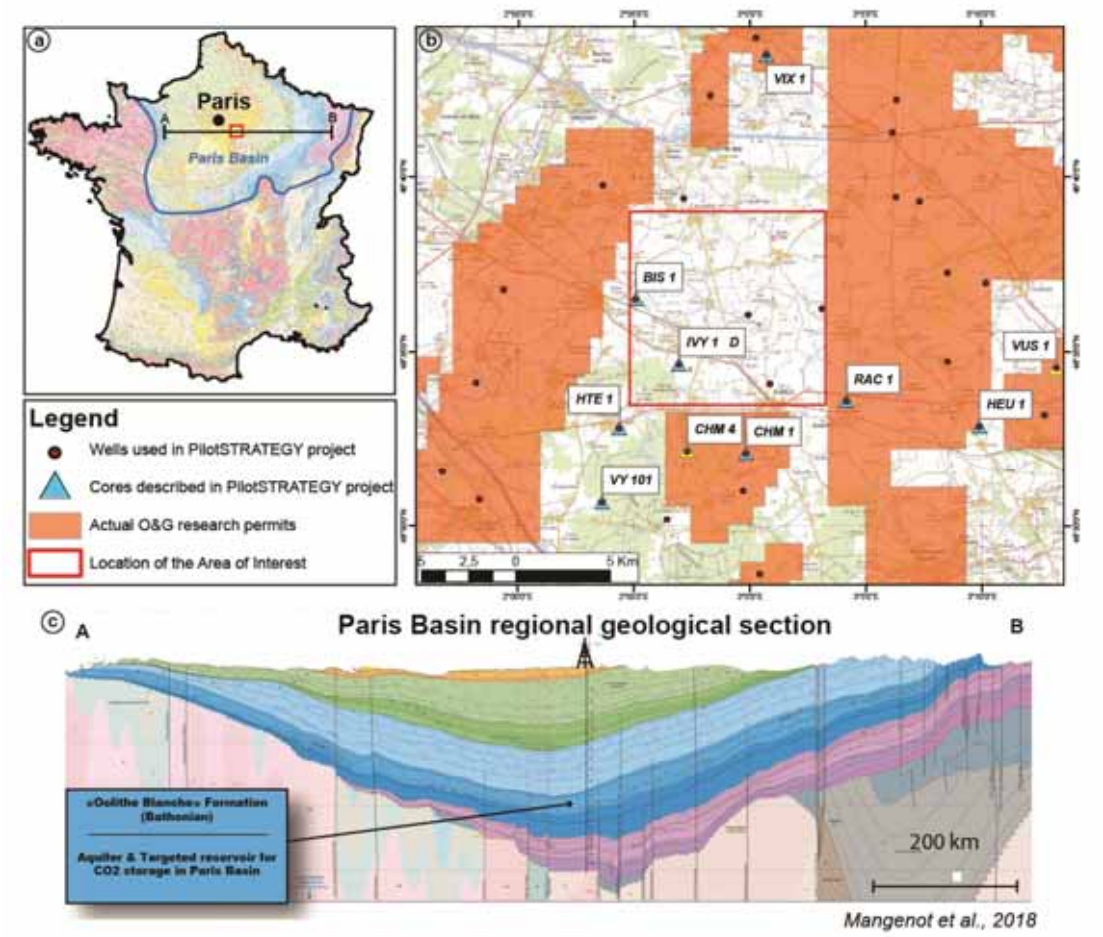

Figure 3-1: Location of the study area and data used in the French area for PilotSTRATEGY project. a) French geological map of France (1:1 000 000) showing location of the study area and the geological section presented in c). b) Location map of the study area and data used in PilotSTRATEGY project. c) Geological section from Paris Basin, showing location of the targeted reservoir in PilotSTRATEGY project. Geological section from Mangenot et al., 2018.

The PilotSTRATEGY project has received funding from the European Union's Horizon 2020 research and innovation programme under grant agreement No. 101022664

One of the features of cores drilled in the area is the poor representation of the target reservoir. During oil exploration, coring was only conducted on the Callovian transgressive deposits. Consequently, only the topmost part of the targeted reservoir is cored and it is known from regional studies that this specific part of the reservoir has poor reservoir properties compared to rest of the formation.

Consequently, a sampling strategy has been conducted with the objective of having a better understanding of the reservoir property variations and how they depend to sedimentary facies; using well log data. This strategy is also adopted due to the small number of samples analysed for Petrophysical study. Sampling strategy is based on:

- Wells, which cores reach the deepest part of the Oolithe Blanche Formation
- Cores, which samples can be taken without damage to the core integrity. This is linked to previous systematic sampling conducted by Petroleum Company during exploration stage.
- Cores, which sampled an important sedimentary facies. This allowed us to understand which facies drive the good reservoir properties of the Oolithe Blanche Formation as well as which facies would have sealing properties.
- Well logs, which show important reservoir properties variations through the same sedimentary facies. This is dedicated to understand the role of diageneses in the Oolithe blanche.

After a screening of all cores described in the project, using the criteria of the sampling strategy, two wells have been selected for sampling: Charmottes 4 (CHM4) and Vulaines-1 (VUS1). Unfortunately, these cores are located slightly outside of the area of interest (AOI). However, because of the homogenous and low heterogeneity of sedimentary units at the local scale, and the absence of good representative cores in the AOI, CHM4 and VUS 1 cores are the best samples for our study.

3.1.2 Charmotte 4 cores and samples

Charmottes-4 well is located at 2 Km south of the Area of Interest (Fig. 31b). From depth -1790 to -1826m (TVD), 36 meters of the sedimentary pile have been cored with a 95% recovery. Stratigraphic interval correspond to:

- Dalle Nacrée Formation: Callovian transgressive system tract with development of isolated oolitic shoals. It corresponds to the oil reservoir targeted during exploration and poor hydrocarbon accumulations were found.
- Comblanchien Formation: latest Bathonian lagoonal facies, which correspond to the downward shift of the Oolitic ramp at the end of the Bathonian. In our study, this interval is interpreted as a relative low-permeable interval, despite very local and small scale permeable layers related to diagenesis and fracturing.
- Oolithe Blanche: Bathonian oolitic ramp that corresponds to the CCS reservoir target. Two main depositional environments are defined in the top reservoir interval with well-developed oolitic shoals and back-barrier facies (bioclastic packstone).

Six samples have been chosen from the Charmottes 4 cores. The Table below indicates for each samples:

- Samples location in the well (core number ; core section ; depth ; stratigraphic interval)
- Unique sample code number
- Type of analyses for sample

The PilotSTRATEGY project has received funding from the European Union's Horizon 2020 research and innovation programme under grant agreement No. 101022664

- Main lithology
- Purpose of the sampling

Results will be presented in sections 3.2 and 3.3

3.1.3 Vulaines-1 cores and samples:

Drilled in 1978, Vulaine-1 well is located at 11 Km east to the Area of Interest (Fig. 1b). From depth -1819 to -1919m (TVD), 100 meters of the sedimentary pile have been cored. Compared to Charmottes-4 well, recovery is under 60% with only 57m thick preserved and described in our study. Stratigraphic interval identified in Vulaines-1 cores correspond to:

- "Marnes de Massangis" Formation: Callovian caprock. This formation corresponds to the proper seal of the reservoir system. It is indurated marls with calcareous nodules.
- Dalle Nacrée Formation: Callovian transgressive system tract with the development of isolated oolitic shoals. It is characterised by meter-thick coarsening upward sequence of oo-bioclastic Grainstone in Vulaines-1 well.
- Comblanchien Formation: represented in Vulaines-1 well by oncolitic and coral rich wackstones and packstones. This formation representa s shallow water environment recording an important regressive stage at the end of Bathonian.
- Oolithe Blanche: Bathonian oolitic ramp that correspond to the reservoir targeted. Due to relative low core penetration of the formation, only two main depositional environments are defined in the top reservoir interval with well-developed oolitic shoals and back-barrier facies (bioclastic packstone).

Six samples have been chosen in Vulaines-1 cores. Details of spreadsheets entries are explained in the section 3.1.2.

The PilotSTRATEGY project has received funding from the European Union's Horizon 2020 research and innovation programme under grant agreement No. 101022664

Table 3-1: List of samples taken and analysed in Charmottes-4 cores

Core	section	Depth	Lithology	Sample Name	Purpose	Interval
2	2/18	1809,5	Oobioclastic GST with cm-thick brahiopods and bivalves clast	CHM4_C2_1809,5	Reservoir properties of Oolithe Blanche : reservoir targeted (coarse-grained oo-bioclastic shoal)	DOGGER RESERVOIR
2	3/18	1811,7	Bioclastic PST/GST with gasteropods, brachiopods, bivalves	CHM4_C2_1811,7	Reservoir properties of Oolithe Blanche : reservoir targeted (back-barrier facies with stylolites)	
2	5 / 18	1812,4	Oolitic Grainstone	CHM4_C2_1812,4	Reservoir properties of Oolithe Blanche : reservoir targeted (oolitic shoal)	
3	9 / 18	1815,9	PST/GST with pelloids, and brachiopods, bioclast and bivalves clasts	CHM4_C2_1815,9	Reservoir properties of Oolithe Blanche : reservoir targeted (back-barrier facies)	
2	15 / 18	1822,1	Oobioclastic GST with corals and bivalves clast. Dunes stratifications	CHM4_C2_1822,1	Reservoir properties of Oolithe Blanche : reservoir targeted (oolitic shoal with specific well logs results)	
2	17 / 18	1824,8	Oolitic GST with cm-thick bioclastic layers and inclined stratifications	CHM4_C2_1824,8	Reservoir properties of Oolithe Blanche : reservoir targeted (oolitic shoal with specific well logs results)	

The PilotSTRATEGY project has received funding from the European Union's Horizon 2020 research and innovation programme under grant agreement No. 101022664

Table 3-2: List of samples taken and analysed in Vulaines-1 cores

Core	Section	Depth	Lithology	Sample Name	Purpose	Interval
6	4/11	1843,45	Argillaceous wackstone with large brachiopods, rare oolites. Extremely bioturbated.	VUS1_c6_1843,45	Reservoir properties at the Caprock / reservoir Transistion: internal seal (lagoonal facies)	
6	5/11	1844,05	Argillaceous wackstone with large brachiopods, rare oolites. Extremely bioturbated.	VUS1_c6_1844,05	Reservoir properties at the Caprock / reservoir Transistion: internal seal (lagoonal facies)	
10	1/8	1891,80	very well sorted oolitic Grainstone passing to oo-bioclastic megaripples	VUS1_c10_1891,8	Reservoir properties of Oolithe Blanche : reservoir targeted (specific sedimentary facies)	DOGGER RESERVOIR
10	6/8	1896,5	Megaripples with oo-bioclastic Grainstone : poorly rounded surficial oolites, echinoderms, “gravelles”, lamellibranches	VUS1_c10_1896,5	Reservoir properties of Oolithe Blanche : reservoir targeted (specific sedimentary facies – oolitic shoal)	
11	3/10	1911,2	Oobioclastic Grainstone passing to planar laminated Oolitic Grainstone	VUS1_c11_1911,2	Reservoir properties of Oolithe Blanche : reservoir targeted (specific sedimentary facies)	
11	9/10	1917	Oblique laminations in Oobioclastic facies	VUS1_c11_1917	Reservoir properties of Oolithe Blanche : reservoir targeted (specific sedimentary facies – oolitic shoal)	
11	10/10	1918	Very well sorted Oobioclastic Grainstone. Bioclasts are not dissolved and correspond to brachiopods & echinoderms fragments.	VUS1_c11_1918	Reservoir properties of Oolithe Blanche : reservoir targeted (specific sedimentary facies)	

The PilotSTRATEGY project has received funding from the European Union’s Horizon 2020 research and innovation programme under grant agreement No. 101022664

3.2 Geomechanical measurements: results

The purpose of the geomechanical measurements is to supply the parameters for the geomechanical model. The model developed by IFPEN needs the elastic and plastic properties laws followed by the elastic and plastic properties of formations as a function of the porosity.

For this purpose, 3 types of tests were conducted (test methodologies are explained in appendix 8):

- Ultrasonic velocity measurements with piezoelectric transducers, for dynamic elastic moduli measurement on unconfined samples.
- Brazilian tests with mechanical press for Tensile strength (UTS) measurement.
- Uniaxial compression tests for Uniaxial compressive strength (UCS) measurement; Static elastic moduli measurement could also be done with strain measurement (with gauge or camera): K (bulk modulus) and G (shear modulus).

To ensure the representativeness of tests, samples must have dimension at least 10 times larger than the "mineral" grains. For these geomechanical tests, we used cylindrical samples, mainly redrilled from the samples used for petrophysical measurements (Deliverable 2.6). Indeed, since the petrophysics tests were favored, the Brazilian and uniaxial compression tests, which are destructive, have been made at the end, on sample that do not have the optimal dimensions and shape.

The measurement results are limited in number because there were few samples and on some, the interpretation of the measurement was impossible:

- Ultrasonic measurement imposed that wavelength must be approximately 10 times over heterogeneity and approximately 10 times smaller the sample length. These measures are relatively simple to perform and have been made on all the samples taken.
- In UTS the sample should respect length (L) greater than diameter (D). Six samples underwent these tests.
- For UCS tests, samples must have L/D > 2; the samples' ends must be smooth and must be perpendicular to the sample axis with a maximum deviation of only 0.06 degrees. Eight samples underwent these tests. Uniaxial compressive stress could be measured, whereas the elastic modulus could not be measured on any sample, mainly because the lack of parallelism prevents a correct interpretation.

The results are given in Table 3-3:

- Sample are named after the core from which they were sampled.
- A core name appears several times, when sample has been redrilled, for measurement purpose (as specified in Table 3-3).
- Velocities have been measured on all the samples, and associated with density, they are interpreted in elastic modulus.
- Brazilian and uniaxial compression results are given for the samples where these tests were possible.

The results are illustrated in Figure 3-2 for Charmottes and in Figure 3-3 for Vulaines, and elastic properties of the two wells are finally compared to the carbonate model used at IFPEN in Figure 3-4. On this figure, it can be observed that the Charmottes samples follow the model, while the Vulaines samples have weaker mechanical properties. Indeed, wave speeds measured on Vulaines samples are

The PilotSTRATEGY project has received funding from the European Union's Horizon 2020 research and innovation programme under grant agreement No. 101022664

generally lower, and this is usually linked to the presence of microcracks (this can be validated by petrographic observation of thin sections).

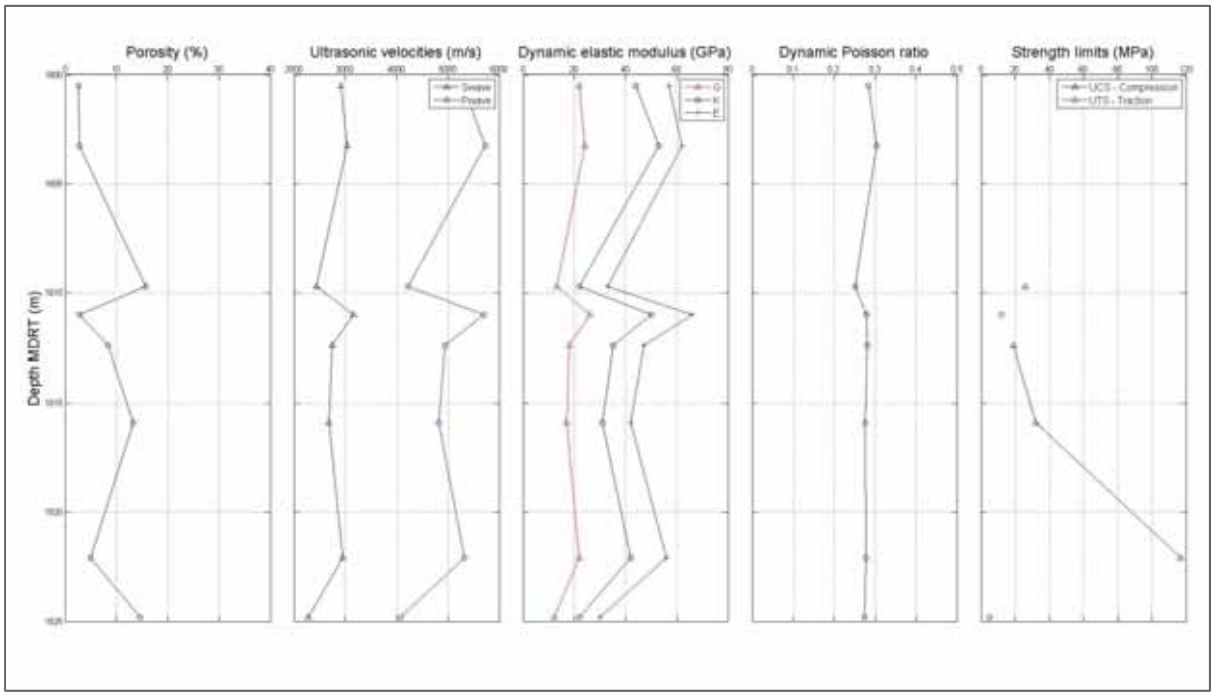

Figure 3-2: Geomechanical results – CHM4

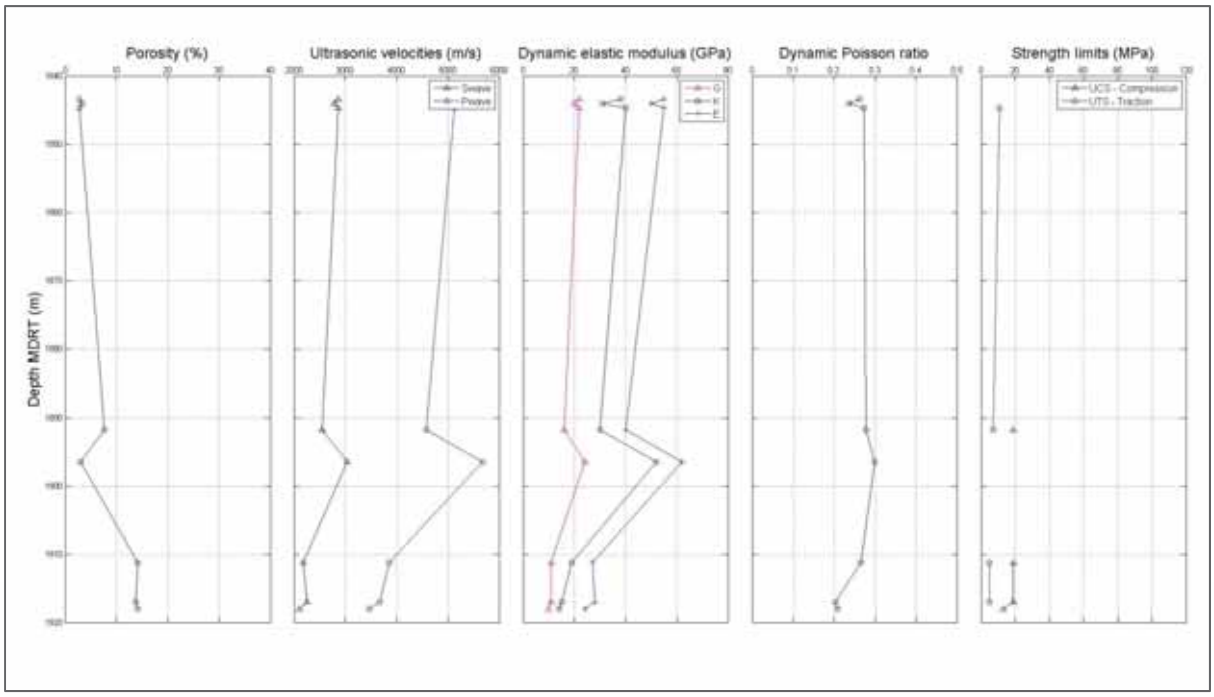

Figure 3-3: Geomechanical results – VUS1

The PilotSTRATEGY project has received funding from the European Union's Horizon 2020 research and innovation programme under grant agreement No. 101022664

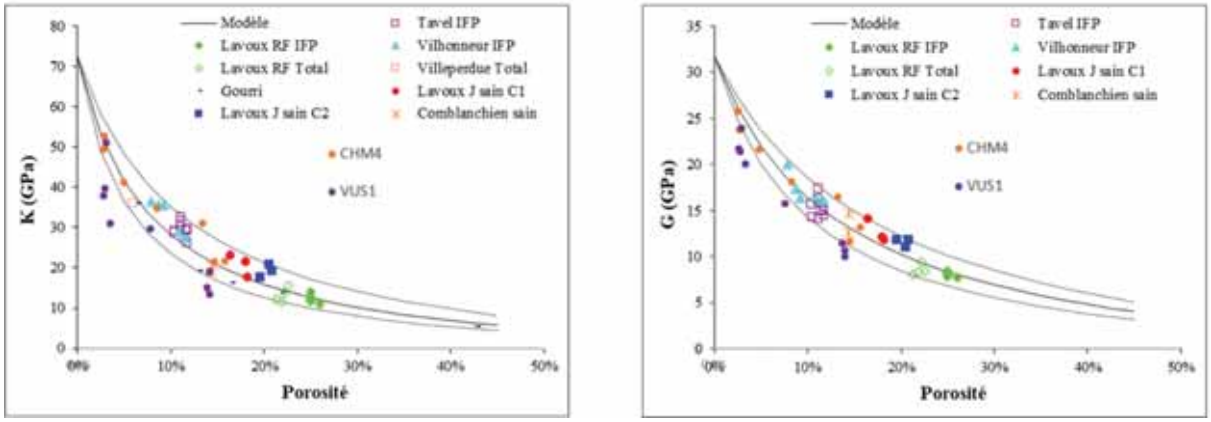

Figure 3-4: CHM4 and VMS1 – K (bulk modulus) and G (shear modulus) results obtain with “impetus” data on dry original plugs (not redrilled ones in Table 3-3), compared to carbonates model (Bemer et al. 2010, Bemer et al. 2004).

The PilotSTRATEGY project has received funding from the European Union’s Horizon 2020 research and innovation programme under grant agreement No. 101022664

Table 3-3: Geomechanical data measured on samples from CHM4 and VUS1

				AIR													SAUMURE (25g/l)													UC test	Brazilian test
					Impetus						Phase							Impetus						Phase							
	Coming from	Ref IFP (Petra)	Porosity (%)	Density (kg/m3)	Vpi (m/s)	Vsi (m/s)	K (GPa)	G (GPa)	E (GPa)	ν	Vpφ (m/s)	Vsφ (m/s)	K (GPa)	G (GPa)	E (GPa)	ν	Density (kg/m3)	Vp (m/s)	Vs (m/s)	K (GPa)	G (GPa)	E (GPa)	ν	Vp (m/s)	Vs (m/s)	K (GPa)	G (GPa)	E (GPa)	ν	UCS (MPa)	Rt (MPa)
CHM4	CHM4_C1_1800.5	4856	2.6%	2 620	5293	2911	44	22	57	0.283	5049	2855	38	21	**54**	0.265	2 646	5326	2678	50	19	51	0.331	4884	2592	39	18	46	0.304		
CHM4	CHM4_C1_1803.25	4857	2.8%	2 592	5729	3038	53	24	62	0.304	5295	2963	42	23	**58**	0.272	2 620	5981	2980	63	23	62	0.335	5702	2916	55	22	59	0.323		
CHM4	CHM4_C2_1809.7	4859	15.7%	2 228	4219	2432	22	13	33	0.251	3994	2336	19	12	**30**	0.240	2 387	4393	2353	28	13	34	0.299	4185	2235	26	12	31	0.300	26	
CHM4	CHM4_C2_1811	4860	2.7%	2 607	5696	3153	50	26	66	0.279	5471	3020	46	24	**61**	0.281	2 634	5892	3068	58	25	65	0.314	5592	2950	52	23	60	0.307		12
CHM4	CHM4_C2_1812.4	4861	8.4%	2 429	4948	2737	35	18	47	0.280	4597	2692	28	18	**44**	0.239	2 514	5289	2705	46	18	49	0.323	4945	2672	38	18	46	0.294		
CHM4	CHM4_C2_1815.9	4862	13.3%	2 302	4822	2682	31	17	42	0.276	4648	2611	29	16	**40**	0.269	2 437	4859	2590	36	16	43	0.302	4548	2536	30	16	40	0.274		
CHM4	CHM4_C2_1822.1	4863	4.9%	2 498	5320	2950	42	22	56	0.278	5156	2867	39	21	**52**	0.276	2 547	5417	2832	48	20	54	0.312	5202	2828	42	20	53	0.290		
CHM4	CHM4_C2_1824.8	4864	14.6%	2 259	4071	2272	22	12	30	0.274	3605	2201	15	11	**26**	0.203	2 407	4584	2269	34	12	33	0.338	4068	2145	25	11	29	0.307		5
VUS1	VUS1_C6_1843.45	4866	2.7%	2 659	5038	2863	38	22	55	0.262	4694	2785	31	21	**51**	0.228															
VUS1	VUS1_C6_1844.05	4867	3.4%	2 611	4725	2778	31	20	50	0.236	4438	2593	28	18	**44**	0.241	2 646	5326	2495	53	16	45	0.359	4705	2457	37	16	42	0.313		
VUS1	VUS1_C6_1844.7	4868	2.8%	2 622	5126	2864	40	22	55	0.273	4686	2708	32	19	**48**	0.249	2 651	5515	2934	50	23	59	0.303	5060	2811	40	21	53	0.277		11
VUS1	VUS1_C10_1891.8	4870	7.7%	2 451	4574	2541	30	16	40	0.277	3831	2371	18	14	**33**	0.190	2 529	5552	2718	53	19	50	0.342	4881	2703	36	18	47	0.279		
VUS1	VUS1_C10_1896.5	4871	3.0%	2 602	5672	3039	52	24	62	0.299	5458	2957	47	23	**59**	0.292	2 632	5851	3075	57	25	65	0.309	5509	2935	50	23	59	0.302		
VUS1	VUS1_C11_1911.2	4873	14.1%	2 263	3854	2175	19	11	27	0.266	3291	2138	11	10	**23**	0.135	2 406	4415	2154	32	11	30	0.344	3898	2135	22	11	28	0.286		
VUS1	VUS1_C11_1917	4874	13.8%	2 280	3675	2246	15	11	28	0.202	3108	2064	9	10	**21**	0.106	2 419	4519	2280	33	13	33	0.329	3893	2126	22	11	28	0.288		
VUS1	VUS1_C11_1918	4875	14.1%	2 263	3467	2105	14	10	24	0.208	2803	1934	6	8	**18**	0.046	2 406	4465	2097	34	11	29	0.359	3799	1984	22	9	25	0.312		
redrilled - plug	CHM4_C2_1812.4	4861-1	8.4%	2 428	4759	2645	32	17	43	0.277	4551	2385	32	14	36	0.311														19	
redrilled - plug	CHM4_C2_1815.9	4862-1	13.3%	2 311	4819	2655	32	16	42	0.282	4636	2645	28	16	41	0.259														32	
redrilled - plug	CHM4_C2_1822.1	4863-1	4.9%	2 487	5222	2895	40	21	53	0.278	5178	2872	39	21	52	0.278														117	
redrilled - plug	VUS1_C10_1891.8	4870-1	7.7%	2 440	4300	2393	26	14	36	0.276	3770	2264	18	13	30	0.218														19	
redrilled - plug	VUS1_C11_1911.2	4873-1	14.1%	2 195	3566	1905	17	8	21	0.300	3276	1583	16	6	15	0.348														19	
redrilled - plug	VUS1_C11_1917	4874-1	13.8%	2 217	2849	1690	10	6	16	0.229	2473	1650	6	6	13	0.099														19	
redrilled - plug	VUS1_C11_1918	4875-1	14.1%	2 267	3217	1810	14	7	19	0.268	2616	1580	8	6	14	0.213														13	
redrilled - plug	VUS1_C10_1891.8	4870-2	7.7%	2 440	4010	2283	22	13	32	0.260	3350	2189	12	12	26	0.127															7
redrilled - plug	VUS1_C11_1911.2	4873-2	14.1%	2 195	3637	1903	18	8	21	0.312	3124	1719	13	6	17	0.283															5
redrilled - plug	VUS1_C11_1917	4874-2	13.8%	2 217	3246	1650	15	6	16	0.326	2815	1630	10	6	15	0.248															5

The PilotSTRATEGY project has received funding from the European Union's Horizon 2020 research and innovation programme under grant agreement No. 101022664

3.3 References

Bemer E. and J.M. Lombard J.M. (2010), From Injectivity to Integrity Studies of CO2 Geological Storage, OGST, Vol. 65.

Bemer E., et al (2004), Geomechanical Log Deduced from Porosity and Mineralogical Content, OGST, Vol. 59

Catinat M., Fleury M., Brigaud B., Antics M., Ungemach P. (2023), Estimating permeability in a limestone geothermal reservoir from NMR laboratory experiments, Geothermics, in revision.

Vincent, B., Fleury, M., Santerre, Y., & Brigaud, B. (2011). NMR relaxation of neritic carbonates: An integrated petrophysical and petrographical approach. Journal of Applied Geophysics, 74(1), 38–58.

The PilotSTRATEGY project has received funding from the European Union's Horizon 2020 research and innovation programme under grant agreement No. 101022664

4. Samples from Spain – On Shore

4.1 Geological aspects. Sampling.

The Spanish onshore study area is located in the Lopín Structure (Zaragoza, Ebro basin) (Figure 4-1). Rock samples for petrophysical (and geomechanical) characterization were obtained from two different sources: 1) samples from stratigraphic sequences studied in natural outcrops (Torre de las Arcas section and Peñas Royas section); and 2) samples from rock cores (Chiprana well) stored at the Rock Sample Storage Centre (IGME-CSIC).

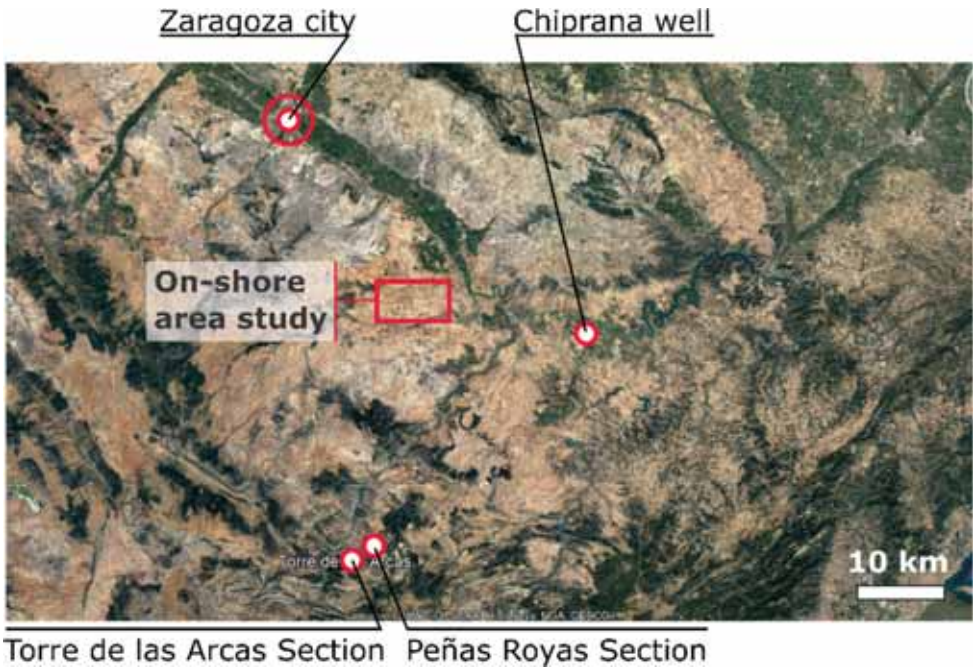

Figure 4-1. Location of the on-shore area study and the Chiprana well as well as the outcrops where both the Torre de las Arcas and Peñas Royas sections are described.

Both natural outcrops (Torre de las Arcas and Peñas Royas) are located 55 km south of the study area (Lopín structure). They are extensive outcrops where a complete stratigraphic sequence of both the reservoir and the seal rock formation can be studied and sampled. Even though rocks exposed in natural outcrops are affected by subaerial weathering processes and, consequently, the petrographic characteristics of these exhumed rocks can be slightly different than the buried materials, these natural outcrops have been considered in this project because of two main reasons:

1. A unlimited number of samples can be taken
2. Large-scale stratigraphic structures can be observed that are not visible in borehole core

The Chiprana well is located 30 km east of the study area. 90 m of rock core of the reservoir formation is preserved at the Rock Sample Storage Centre (IGME-CSIC).

The PilotSTRATEGY project has received funding from the European Union's Horizon 2020 research and innovation programme under grant agreement No. 101022664

Stratigraphic Units.

Proposed reservoir and seal rocks are a sedimentary sequence formed by The Buntsandstein Facies. The Buntsandstein predominantly consists of red sandstone layers of the Lower Triassic series and is one of three characteristic Triassic units, together with the Muschelkalk and Keuper that form the Germanic Triassic Supergroup.

The reservoir is identified as the Tierga Fm, which is divided in the Aranda, Carcalejos and Rané members. They are composed mainly of sandstones with intercalations of shales of variable thickness, which tend to be thicker towards the top (Rané Mb). It also contains some levels of conglomerates, which usually appear between the base and middle areas of the unit. They have been interpreted as fluvial channels braided in intermediate zones of alluvial fans that pass vertically to distal deposits and finally a tidal deltaic system (Arribas, 1984). More recently there are parts that have been interpreted as erg deposits (Soria et al., 2009). The average thickness of the Tierga Fm in the area is around 120 m.

Seal rocks are formed by the Cálcena Fm, which is composed by red shales with some sandstone intercalations towards the base, green marls, gypsum/anhydrites, and dolomites. Towards the top, the carbonate and gypsum content increases. In the field, it shows pseudomorphs of evaporites and tepee structures. Its thickness varies from 10 to 70 m, and the contacts with both the lower and upper formations are gradual and concordant.

Samples

75 samples were taken in all (see table below). Conventionally, samples from natural outcrops are irregular in shape of decimetre scale. However, due to exceptional accessibility in the Torre de las Arcas outcrop, small regular cores were taken with a portable core drill. These cores are cylindrical samples with 5.5 cm in diameter and up to 10 cm in length. Only the strongest and most cohesive levels were sampled with the portable core drill.

In addition, 10 samples were taken from the Chiprana well. Due to the strict regulations of the Rock Sample Storage Centre (IGME-CSIC), only small samples of the most representative levels have been obtained.

The total number of stratigraphic levels sampled in each section and the total number of rock samples taken is indicated in Table 4-1.

Table 4-1. Stratigraphic levels sampled in each section

	Stratigraphic levels	
	Sampled	Total Number of samples
Torre de las Arcas Section	12	44
Peñas Royas Section	11	21
Chipriana Section	10	10

4.1.1 Torre de las Arcas Section

Torre de las Arcas section is a stratigraphic sequence studied in a large outcrop located in the Gabardal Valley, close to the Torre de las Arcas town (Teruel, Spain) (Figure 4-1). 44 samples were taken from Torre de las Arcas Section, corresponding to 12 representative stratigraphic levels (Table 4-2). 10 samples of red quartz-arenite with planar and trough cross-stratification or with lamination of ripples

The PilotSTRATEGY project has received funding from the European Union's Horizon 2020 research and innovation programme under grant agreement No. 101022664

were analysed. The table below shows the complete list of samples. Three samples from the seal formation were composed of silts, clays, and marls and many pseudomorphs of gypsum were analysed. A Hyphen in Table 4-2 indicates flat and slab samples.

Table 4-2. Samples taken from Torre de las Arcas Section.

Reservoir/Seal	Sampled stratigraphic levels	Number of samples irregular	cores	Samples code
Reservoir	PS.TA.01		6	01A; 01B; 01C; 01D; 01E; 01F
Reservoir	PS.TA.02		7	02A; 02B; 02C; 02D; 02E; 02F; 02G
Reservoir	PS.TA.03		4	03A; 03C; 03D; 03F
Reservoir	PS.TA.04		3	04A; 04B; 04C
Reservoir	PS.TA.05	2, -		
Reservoir	PS.TA.06	2, -		
Reservoir	PS.TA.07	-*		
Reservoir	PS.TA.08	1		
Reservoir	PS.TA.09	5		
Reservoir	PS.TA.10	11		
Seal	PS.TA.11	-*		
Seal	PS.TA.12	-*		
Seal	PS.TA.13	3		

* Non-cohesive and crumbly samples

4.1.2 Peñas Royas Section

The Peñas Royas section is a stratigraphic sequence studied in an extensive outcrop located in Martin River Cultural Park, near Peñas Royas village (Teruel, Spain) (Figure 4-1). 21 samples were taken from the Peñas Royas Section, corresponding to 11 representative stratigraphic levels (Table 4-3). The table below shows the complete list of samples. The samples of the reservoir formation (Tierga Fm) are composed of red quartz-arenites with quartz and Fe-oxide cements, with cross-stratification or with ripple lamination of the . Three samples from the seal formation composed of silts, clays and marls were analysed. Asterisk in Table 4-3 indicates non-cohesive and crumbly samples. Hyphen in Table 4-3 indicates flat and slabs samples.

Table 4-3. Samples taken from Peñas Royas section.

Reservoir/Seal	Sampled stratigraphic levels	Number of samples
Reservoir	PS.PR.01	9
Reservoir	PS.PR.02	1
Reservoir	PS.PR.03	1
Reservoir	PS.PR.04	-
Reservoir	PS.PR.05	2
Reservoir	PS.PR.06	-
Reservoir	PS.PR.07	- *
Reservoir	PS.PR.08	3
Seal	PS.PR.09	2
Seal	PS.PR.10	2
Seal	PS.PR.11	1

* Non-cohesive and crumbly samples

The PilotSTRATEGY project has received funding from the European Union's Horizon 2020 research and innovation programme under grant agreement No. 101022664

4.1.3 Chiprana Section

--This stratigraphic section has been studied from well cores available at the Rock Core Storing Centre (IGME-CSIC). A complete 90 m of rock cores from the Chiprana well preserves the reservoir formations studied in this project. 10 samples were taken Chiprana Section, corresponding to 10 representative stratigraphic levels (Table 4-4). The samples of the reservoir formation are composed of red quartzarenites with cross-stratification and red silts with fine ripple lamination. Table 4-4 shows the complete list of samples.

Table 4-4. Samples taken from Chiprana Section

Reservoir/Seal	Sampled stratigraphic levels	Number of samples
Reservoir	CH.1743	1
Reservoir	CH.1747	1
Reservoir	CH.1752	1
Reservoir	CH.1758	1
Reservoir	CH.1764	1
Reservoir	CH.1768	1
Reservoir	CH.1773	1
Reservoir	CH.1788	1
Reservoir	CH.1796	1
Reservoir	CH.1824	1

The PilotSTRATEGY project has received funding from the European Union's Horizon 2020 research and innovation programme under grant agreement No. 101022664

4.2 Geomechanical measurements: results

A complete geomechanical characterization was carried out on the Torre de las Arcas section. Mechanical strength, tensile strength and both static and dynamic elastic modulus were obtained following the conventional tests: Uniaxial Compressive Strength test (UCS), Brazilian test, Ultrasounds and Strain Gauges.

The main results were obtained from the cores sampled in the Torre de las Arcas outcrop with the portable core drill. However, these cores only were obtained from the four most tough rock levels. To check the mechanical properties of the whole sedimentary section, including both tough and weak rock levels, other non-conventional methods have been applied (Schmidt Rebound Hammer and Point Load Test).

Reference values (average values) for the proposed reservoir rock are shown in Table 4-5.

Table 4-5. Mean value of the calculated mechanical properties of the proposed reservoir rock. All the samples of Torre de las Arcas section are considered.

Rock mechanics property	Units	Average value
Uniaxial compression strength (σ_{UCS})	MPa	83.16
Tensile strength (σ_t)	MPa	7.22
Static Young modulus (E_s)	GPa	19.41
Static Poisson coefficient (υ_s)	-	0.33
Ultrasonic P-wave propagation velocity (vp)	Km/s	2.54
Ultrasonic S-wave propagation velocity (vs)	Km/s	1.22
vp/vs	-	1.99
Spatial wave attenuation (α_s)	dB/cm	7.08
Dynamic Young modulus (E_s)	GPa	9.26
Dynamic Poisson coefficient (υ_s)	-	0.33

Table 4-6 shows the obtained compressive strength, tensile strength and static elastic modulus (Young moduli, E_s, and Poisson coefficient, υ_s) measured at laboratory (core samples).

Table 4-6. Mean value and Standard Deviation (SD) of compressive strength, tensile strength, and static elastic modulus of the sampled stratigraphic levels of the Torre de las Arcas section.

	Samples	Compressive strength [MPa]		Tensile strength [MPa]		Static elastic modulus E_s [GPa]		υ_s [-]	
level		mean	SD	mean	SD	mean	SD	mean	SD
1	6	76.00	8.78	4.29	1.19	19.73	1.54	0.31	0.03
2	7	87.03	1.46	7.09	0.76	21.15	1.69	0.39	0.08
3	4	86.44	8.30	8.61	0.07	17.35	2.62	0.30	0.06
4	2			8.90	0.41				

Table 4-7 shows the obtained results in the ultrasounds test: P-wave propagation velocity (vp), S-wave propagation velocity (vs), vs to vp ratio (vp/vs), spatial attenuation of the ultrasonic P-wave (α_s) and the dynamic elastic modulus (Young moduli, E_d, and Poisson coefficient, υ_d). This ultrasounds test was carried out at laboratory (core samples).

The PilotSTRATEGY project has received funding from the European Union's Horizon 2020 research and innovation programme under grant agreement No. 101022664

Table 4-7. Mean value and Standard Deviation (SD) of ultrasonic parameters of the sampled stratigraphic levels of the Torre de las Arcas section.

		Vp [km/s]		Vs [km/s]		vp/vs [-]		α_s [dB/cm]	
level	samples	mean	SD	mean	SD	mean	SD	mean	SD
1	6	2.1	0.11	1.21	0.02	2.07	0.02	9.52	0.70
2	9	2.54	0.34	1.24	0.04	2.04	0.11	6.29	0.83
3	4	2.36	0.26	1.22	0.02	1.93	1.00	5.43	0.87

Table 4-8 shows the dynamic elastic modulus (Young moduli, E_d, and Poisson coefficient, υ_d) measured at laboratory (core samples) from both ultrasonic data (vp and vp/vs) and bulk density determinations.

Table 4-8. Mean value and Standard Deviation (SD) of dynamic elastic modulus of the sampled stratigraphic levels of the Torre de las Arcas section.

		E_s [GPa]		υ_s [-]	
level	samples	mean	SD	mean	SD
1	6	9.07	0.41	0.35	0.01
2	9	9.65	0.61	0.34	0.02
3	4	9.33	0.32	0.32	0.02

Finally, Table 4-9 shows the mechanical strength obtained from indirect measurements (Point Load Test and Schmidt Rebound Hammer). These determinations were carried out directly in natural outcrops (Schmidt Rebound Hammer, σ-r) as well as at laboratory using small irregular samples (Point Load Test, σ-PLT). Rock strength assessed by means of Schmidt Rebound Hammer was assessed following two different procedures: those proposed by ISRM (σ-r(ISRM)) and by ASTM (σ-r(ASTM)).

The objective of carrying out these additional tests was to obtain mechanical properties of different stratigraphic levels, including the less cohesive and even crumbly materials. Standard laboratory tests (i.e. uniaxial compression test or Brazilian test) require geometric samples and they can only be taken from tough and cohesive materials.

Table 4-9. Mechanical strength obtained from indirect measurements (Point Load Test and Schmidt Rebound Hammer) in the stratigraphic levels of Torre de las Arcas section.

level	Rock facies	σ-PLT [MPa]		σ-r(ISRM)	σ-r(ASTM)
		Parallel to structure	Perpendicular	[MPa]	[MPa]
0	Sandstone			32.1	27.4
0	Conglomerate	37.9	63.2	23.4	22.0
1	Sandstone	52.2		70.0	51.6
2	Sandstone (base)	30.1		53.7	48.6
2	Sandstone (top)			61.8	47.5
3	Sandstone	54.7	78.8	61.5	43.9
4	Sandstone	95.0	96.7	81.2	60.3
5	Sandstone (X)	34.7	60.2	91.3	59.2
5	Sandstone (//)			60.5	46.1
6	Sandstone (fine)	27.5	37.1	82.3	59.6
7	Siltstone	59.7	95.4	63.8	46.1
8	Sandstone (//)	28.9		48.9	31.4

The PilotSTRATEGY project has received funding from the European Union's Horizon 2020 research and innovation programme under grant agreement No. 101022664

8	Sandstone (X)			42.9	35.0
9	Sandstone (X)	26.5	32.9	59.6	46.1
10	Sandstone	43.7	64.9	70.0	41.7
11	Sandstone	21.4	34.9	54.9	36.3
12	Sandstone (X)	78.1	104.9	72.3	37.3
13	Sandstone	19.0	51.1	91.8	72.0

Significant differences in the mechanical response of rocks were found comparing materials of different sedimentary facies. These differences can reach up to 70 MPa between the weakest to the strongest levels, that suppose a variation of 12% with respect the mean strength value. Moreover, the Point Load Test (PLT values) were determined considering the load direction with respect to the stratigraphic structure of the rock/sample. Rock results significantly stronger when it is loaded perpendicular to the stratigraphic structure (40% higher when it is tested perpendicular to structure, as average value).

The PilotSTRATEGY project has received funding from the European Union's Horizon 2020 research and innovation programme under grant agreement No. 101022664

4.3 References

Arribas, J. (1984). *Estudio petrológico del Pérmico y Triásico de Malanquilla (Rama Aragonesa de la Cordillera Ibérica).* Tesis de Licenciatura, Universidad Complutense de Madrid.

Bear, J.: *Dynamics of fluids in porous media*. Dover publications, New York (1988)

Brunauer, S., Emmett P. H., and Edward Teller (1938). *Adsorption of Gases in Multimolecular Layers*. Am. Chem. Soc., 60, 2, 309–319

Clauser, C. (1992). *Permeability of crystalline rocks*. Eos, Transactions American Geophysical Union, 73(21), 233-238.

Cranganu, C., & Soleymani, H. (2015). *Carbon dioxide sealing capacity: Textural or compositional controls? A case study from the Oklahoma Panhandle*. AAPG/DEG Environmental Geosciences, 22(2), 57-74.

EN-1936:2007, Natural Stone Test Methods, 2007. *Determination of real density and apparent density, and of total and open porosity*. AENOR eCEN, 14 pp.

Hendrickx, R. (2013). *Using the Karsten tube to estimate water transport parameters of porous building materials*. Materials and structures, 46(8), 1309-1320.

Pittman, E. D. (1992). *Relationship of porosity and permeability to various parameters derived from mercury injection-capillary pressure curves for sandstone*. AAPG bulletin, 76(2), 191-198.

Robinson, R. B. (1966). *Classification of reservoir rocks by surface texture*. AAPG Bulletin, 50(3), 547-559.

Schön, J. H. (2015). *Physical properties of rocks: Fundamentals and principles of petrophysics*. Elsevier.

Schowalter, T. T. (1979). *Mechanics of secondary hydrocarbon migration and entrapment*. AAPG bulletin, 63(5), 723-760.

Soria, A., Liesa, C., Rodríguez-López, J., Meléndez, N., de Boer, P., & Meléndez, A. (2011). *An Early Triassic evolving erg system (Iberian Chain, NE Spain):* palaeoclimate implications. *Terra Nova*.

Swanson, B. F. (1981). *A simple correlation between permeabilities and mercury capillary pressures*. Journal of Petroleum Technology, 2498–2504.ASTM D5731 – 95: Standard Test Method for Determination of the Point Load Strength Index of Rock. ASTM International, West Conshohocken, PA.

The PilotSTRATEGY project has received funding from the European Union's Horizon 2020 research and innovation programme under grant agreement No. 101022664

5. Samples from Spain – Off shore

5.1 Geological context

The study area of the Spanish Offshore region for the PilotSTRATEGY Project (See Figure 5-1), has been traditionally explored for hydrocarbons aiming at early Tertiary and Mesozoic carbonates. These units are stratigraphically deeper than the clastic upper Miocene reservoir under evaluation in this project. For that reason most of the available hard data corresponds to the deeper formations, mostly limestones and marls. The only clastic saline aquifer of interest for carbon storage within the AOI are the upper Miocene Castellón Sandstones and the Middle Miocene Salou sandstone.

Figure 5-1 Location Map and Area of Interest (yellow box)

In the Figure 5-2 the Rodaballo-1 well displays the Gamma Ray (GR) log showing the irregular signature in the Castellon Sandstones and the higher GR response, with a more constant character, depicting the sealing facies of the Ebro clays. Secondary clastic plays for carbon storage such as the Salou sandstones are out of the scope of this petrophysical analysis. The lower Miocene and Oligocene section corresponds to the formations developed in the past three decades for the oil and gas industry.

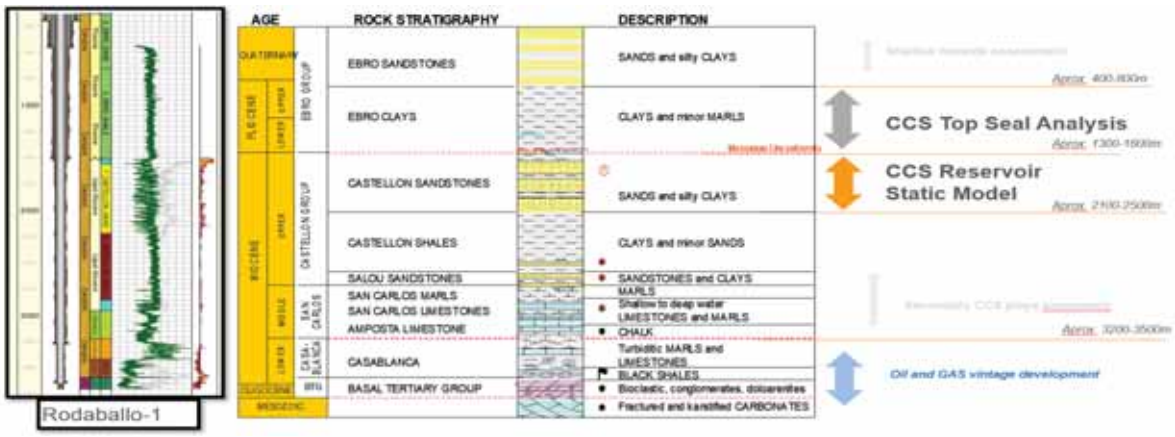

Figure 5-2 Stratigraphic Column and zones of interest Ebro Offshore

The PilotSTRATEGY project has received funding from the European Union's Horizon 2020 research and innovation programme under grant agreement No. 101022664

A 29m reservoir-seal core sample is available from the Amposta Marino C2 well in the AOI, plus 3 core pieces in the Amposta Marino B2 (AB2) and CastellónE-2 (CE2). Several vertical and horizontal plugs have been extracted from the Amposta Marino-C2 core to perform routine core analyses (RCAL). These core samples were sent to the IFPEN and IGME lab facilities. The AB2 and CE2 core pieces are not in an adequate condition to perform the IFPEN analyses (very fragile and or broken) so IGME has made use of them to perform mercury porosimetry analyses.

Figure 5-3 Reservoir Core plugs from wells (left to right) Amposta Marino C-2, Amposta Marino-B2 and Castellón-C1.

Additionally, cuttings set from the well Sardina-1 composed of 12 samples covering reservoir and seal sections has been selected for analysis and has been sent to IGME facilities to perform mercury porosimetry, XRD (X-ray diffraction) analysis and to IFPEN facilities to perform permeability and formation factor, porosity + clay bound water, irreducible water saturation and entry pressure analysis.

Figure 5-4 Cuttings Samples from Sardina-1 well covering seal (Ebro SH) and Reservoir (Castellón SST)

The PilotSTRATEGY project has received funding from the European Union's Horizon 2020 research and innovation programme under grant agreement No. 101022664

5.2 Geomechanical Analysis

Due to the size of the core available in the well Amposta Marino C-2, it was not possible to send 5cm diameter and 12cm length core sample as was requested by IFPEN laboratory for geomechanical analysis. The original objective was performing Brazilian tests to obtain an indirect measurement of the tensile strength, UCS (Unconfined Compressive Stress) to obtain the highest stress that a rock specimen can carry, and static elastic moduli, and dynamic elastic moduli through ultrasounds to obtain the elastic constants.

To cope with this lack of suitable data, the geomechanical rock properties of the prospect have been estimated using the experimental mathematical formulas herein described.

The three main logs to calculate the different parameters are the Density log (DEN), the compressional sonic velocities (DTC) and the shear sonic velocities (DTS).

The density calculation for the entire well column has been derived from the neutron density logs. To obtain density where no density log is available, we extrapolated it from sonic and near surface mathematical correlations (Miller).

When there is lack of shear sonic velocity, we have used the Castagna relationships (Castagna et al 1985) to convert from DTC (compression wave velocity) to DTS (shear wave velocity) utilising some extra wells for calibration of the a and b parameters. The formula is

$$\boldsymbol{DTS\_Castagna} = \left(\frac{\mathbf{1}}{\left(\boldsymbol{a} \times \left(\frac{\mathbf{1}}{\boldsymbol{DTCO}} \times \mathbf{304.8}\right) - \boldsymbol{b}\right)}\right) \times \mathbf{304.8}$$

Units are microseconds/ft and a = 0.98 and b = 1.65. Note that this formula does not apply for limestone horizons.

Observe in Figure 5-5 that in the upper section DTS modelled (dashed red line) calibrates correctly with the acquired DTS (orange line) but in the carbonate section (from Sand Carlos Marls downward) the calibration is not perfect. The Castagna relationships used work better for clastics (sandstones and shales). Since our reservoir of interest is in the shallower section, we can go forward with the curves modelled.

The PilotSTRATEGY project has received funding from the European Union's Horizon 2020 research and innovation programme under grant agreement No. 101022664

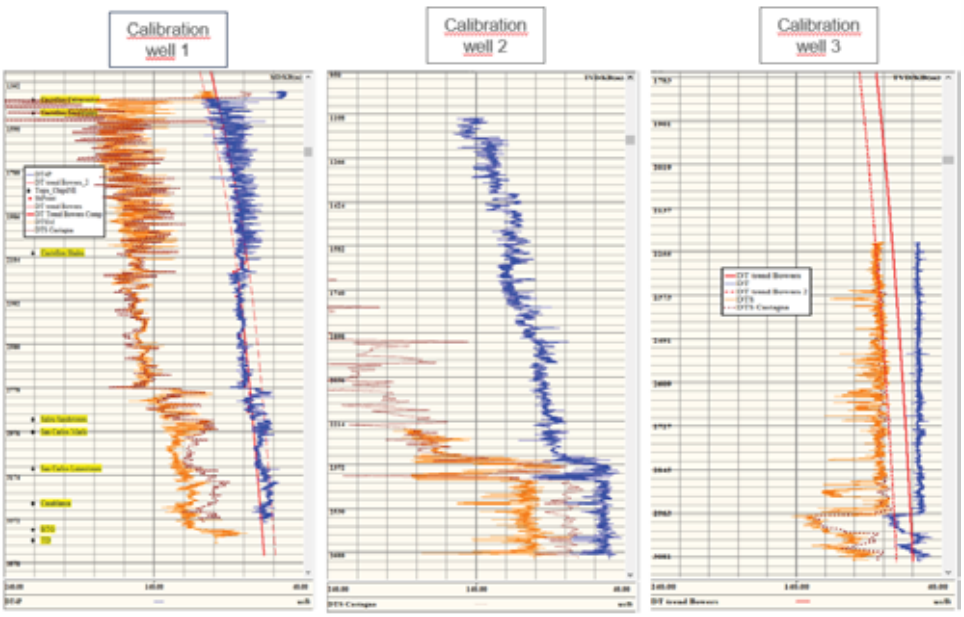

Figure 5-5 Shear Sonic Calibration of the Castagna empirical relationships.

Once the shear velocities are calculated for the objective wells, we can extrapolate Young's modulus (E) with the relationship:

$$E = \rho_b \times Vs^2 \times \frac{3 \times Vp^2 - 4 \times Vs^2}{Vp^2 - Vs^2}$$

The rest of the parameters needed for geomechanical modelling were calculated using the following relationships.

Dynamic Poisson ratio (for clastics):

$$\nu = \frac{Vp^2 - 2 \times Vs^2}{2 \times (Vp^2 - Vs^2)}$$

The static Poisson ration will be the 78% of the dynamic.

Shear Modulus:

$$Gs = \rho_b \times Vs^2$$

Bulk Modulus G:

$$G = \rho_b * \left(Vp^2 - \left(\frac{4}{3} \times Vs^2\right)\right)$$

UCS Clastics:

Sandstone: $UCS = 1200 \times e^{(-0.036 \times DTCO)}$ **(Mc Nally)**

Shale: $UCS = 10 \times \left(\frac{304.8}{DTCO - 1}\right)$ **(Lal modif.)**

Tensile Strength:

$$Ts = 0.1 \times UCS$$

The PilotSTRATEGY project has received funding from the European Union's Horizon 2020 research and innovation programme under grant agreement No. 101022664

5.3 In situ Stress Calculation Methodology

The in-situ stress calculation of the three wells of interest has been performed using the log data available and the next correlations

- Overburden profile:

Performed with Gardner Formula (Gardner, 1974) using density log and Miller formula (1967) when density is absent and the next parameters:

Water density = 1.05g/cc

Rock density at mudline = 1.95g/cc

- Normal Compaction trend using Bower's Formula (Bowers, 1995)

$$V(ft/s) = Vgl(ft/s) + A \times effective\ stress\ (psi/ft)^B$$

Where: Vgl= 6980 ft/s

A= 14.2

B=0.714

Effective stress=0.45 psi/ft

- Pore pressure Calculation using Eaton's Formula

$$PPG = OBG - ((OBG - Pn) \times (DTn\ /\ DTo)^3)$$

$$PPG = OBG - ((OBG - Pn) \times (Vo/Vnormal)^3)$$

where:

PPG = Pore Pressure Gradient

OBG = Overburden Gradient

DTn, Vn= normal shale transit time or velocity from trend line

Dto, Vo= observed shale transit time or velocity

Pn = Hydrostatic Pressure (normal pressure)

- Fracture Gradient Calculation with Mathew's & Kelly Formula calibrated with LOT (Leak off Tests) / FIT (Formation Integrity Test) results.

$$FP = PP + K \times (OBP - PP)$$

Where:

OBP = Overburden Pressure

Pp= Pore Pressure

The PilotSTRATEGY project has received funding from the European Union's Horizon 2020 research and innovation programme under grant agreement No. 101022664

K= Effective stress ratio

FP= Fracture Pressure

LOT= Leak off test Pressure

5.3.1 Amposta Marino C2 Well

In this well, there is data available mostly from the 12 ¼'' & 8 ½'' sections. There is no DTS available (so was calculated from Castagna formula correlation) and no available MW (Mudweight) data so data was used from the AMB2 well. Neither is there an available directional survey (it was hence assumed that this is a vertical well)

The **Ebro Fm** is subdivided in two different intervals:

- **760-1110 mMD**: Silty claystone characterized by "large scale foresets"
- **1110-1560 mMD**: Most uniform plastic claystone and some interbedded sandstone intervals. Some marly invtervals are described. Described as marly clays with interbedded siltstones and limestones levels.

The Castellón Sandstone runs from 1560mMD to 1900mMD and it is described as Sandstones with interbedded shales and occasionally clays. There are some bad Caliper data zones which makes it very difficult to interpret with breakout effects for rock properties/horizontal stress correlation.

The main Drilling Events are

- Ebro Fm.:
    - 20'' casing stuck @ 736 mMD.
- Jurassic:
    - Partial losses (10bbls/m).

The PilotSTRATEGY project has received funding from the European Union's Horizon 2020 research and innovation programme under grant agreement No. 101022664

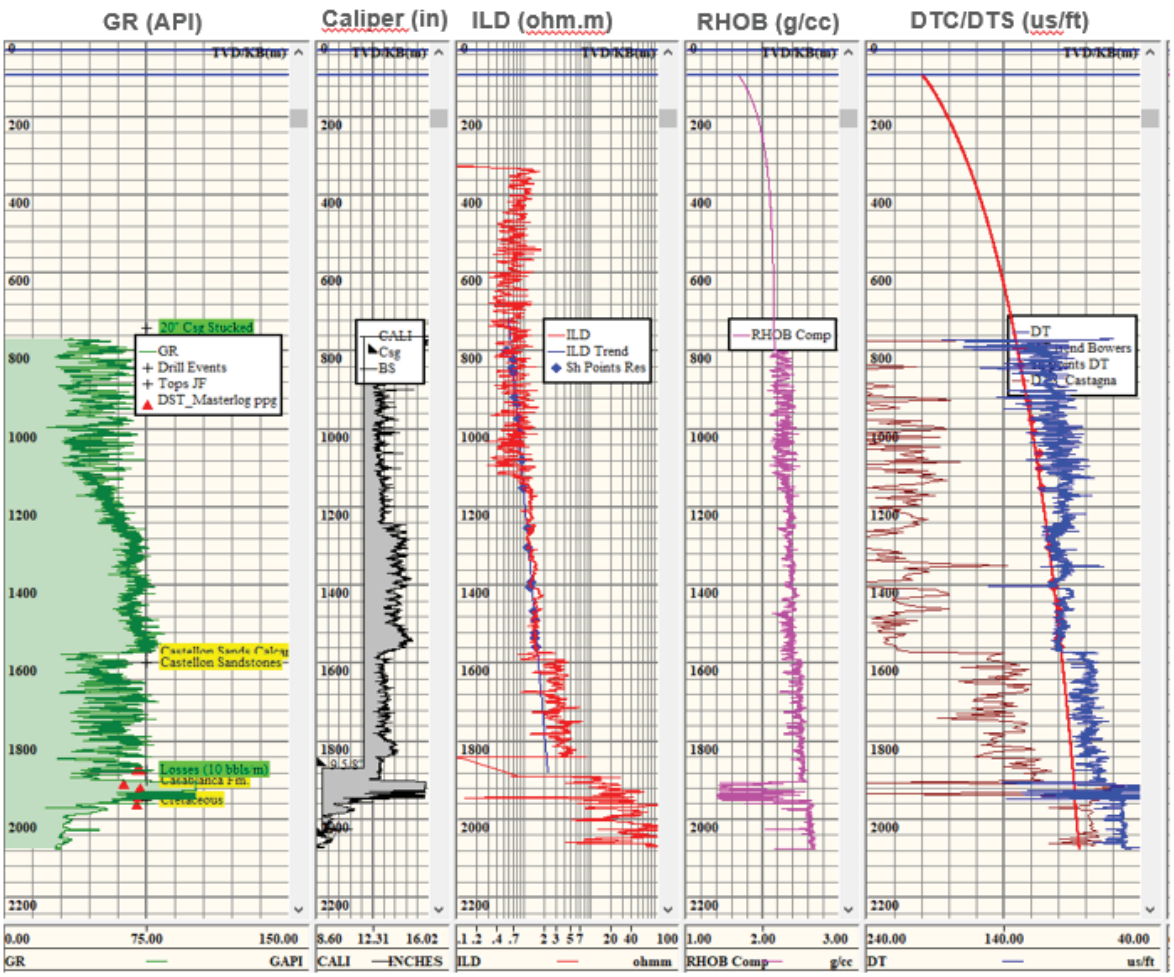

Figure 5-6 Input logs for Amposta Marino C2 well, including the density extrapolation to the surface with Miller's equation (upper pink log) and Shear Sonic Modelled through Castagna relationships (brown log) and in-situ stress calculation.

To calculate the Pore Pressure Fracture Gradient Profiles we have followed the next 4 steps

1. Overburden Profile using Density (g/cc) log up to the surface. To estimate the missing section from 800m to seabed we use the Miller Formula.
2. The Normal compaction trend is estimated using Bowers method before described using the coefficients (A:14.2 & B:0.745)
3. The Pore pressure calculation is obtained through Eaton's formula exp:3 using DTCO and Resistivity logs. Overall the well presents a hydrostatic pressure profile and several calibration points:

   Base Castellon Formation DST: 8.6 ppg Oil & Gas production (72 bbls maximum).

   Max buoyancy at top of Castellon Fm.: 8.8 ppg (assuming 0.85 g/cc oil density) 8.5 ppg (hydrostatic aquifer pressure)

4. We calculate two main cases for fracture gradient prognosis (Mathews & Kelly formula) considering that no FIT (Formation Integrity Test) or LOT (leak-off test) were acquired in this well.

The PilotSTRATEGY project has received funding from the European Union's Horizon 2020 research and innovation programme under grant agreement No. 101022664

- Shmin = 0.4 x ESR (Effective Stress Ratio based on M&K - worst case scenario assuming high carbonaceous content).
- Shmax = 0.6 x ESR M&K (assuming high regional fracture values).

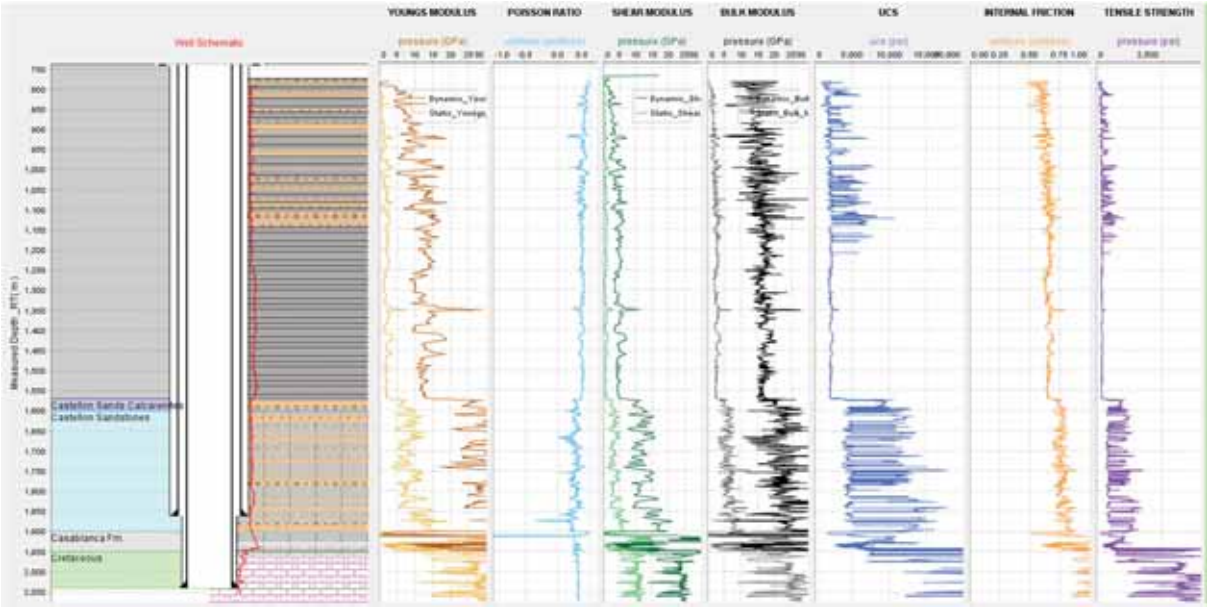

Figure 5-7 Elastic and geomechanical parameters prediction with the empirical relationships presented in the text for the Well Amposta Marino C2.

This analysis of in-situ stress needs to be calibrated. In the absence of hard data, a breakout width has been calculated using LADE methodology and then compared to the caliper. This comparison has helped to choose the appropriate parameters of the UCS estimations modifying the parameter in McNally relationship to:

$$\mathbf{UCS} = \mathbf{900} \times \mathbf{e}^{(-\mathbf{0.036} \times \mathbf{DTCO})}$$

And modifying Lal relationship to:

$$\mathbf{UCS} = \mathbf{10} \times \left(\frac{\mathbf{304.8}}{\mathbf{DTCO} - \mathbf{1}}\right)$$

The PilotSTRATEGY project has received funding from the European Union's Horizon 2020 research and innovation programme under grant agreement No. 101022664

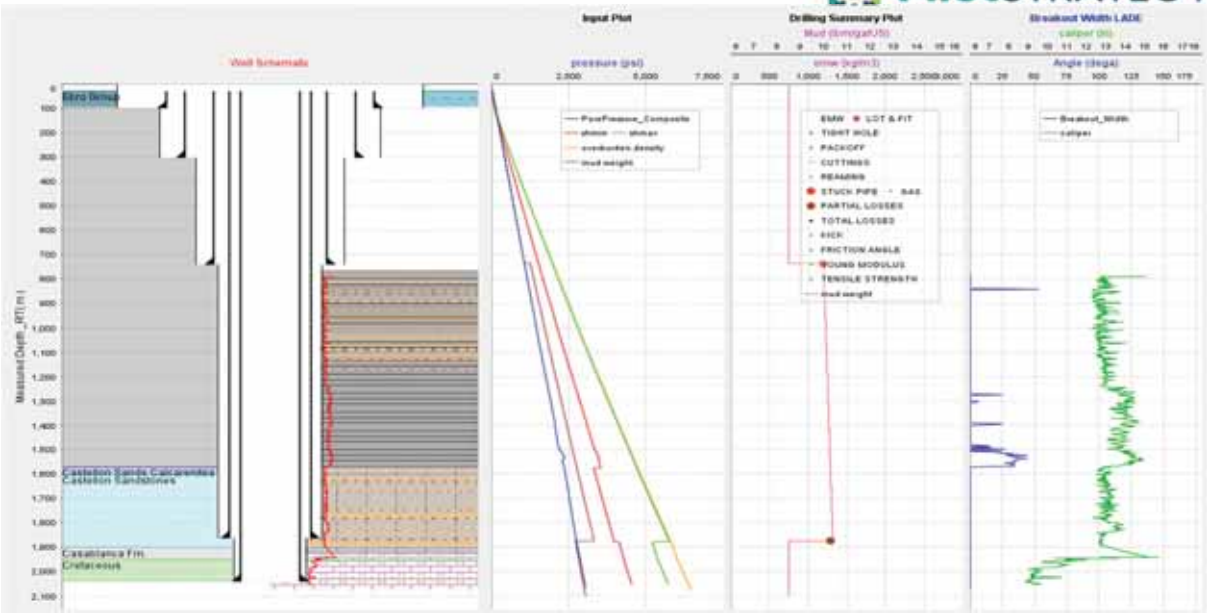

Figure 5-8 *Well Schematic, lithology, in situ stress calculation and breakout analysis of Amposta Marino C2 well to QC the 1D model*

5.3.2 Rodaballo-1 Well

The Rodaballo-1 well did not acquire any DTS (Shear Sonic log) so it was calculated from the Castagna correlation. Since no directional survey is available it is assumed to be a vertical well. Overall the well presents good caliper data and there are two main formations of interest:

- Ebro Shales: described as marly clays with interbedded siltstones and limestones levels.
- Castellón Sandstone: described as Calcarenites on top, Sandstones with interbedded shales and occasionally clays.

There were a couple of Drilling Events according to the Drilling Well Report:

- At Ebro Shales there were some overpull events up to 70klbs.
- At Castellon Sandstone there was a tight hole event

The PilotSTRATEGY project has received funding from the European Union's Horizon 2020 research and innovation programme under grant agreement No. 101022664

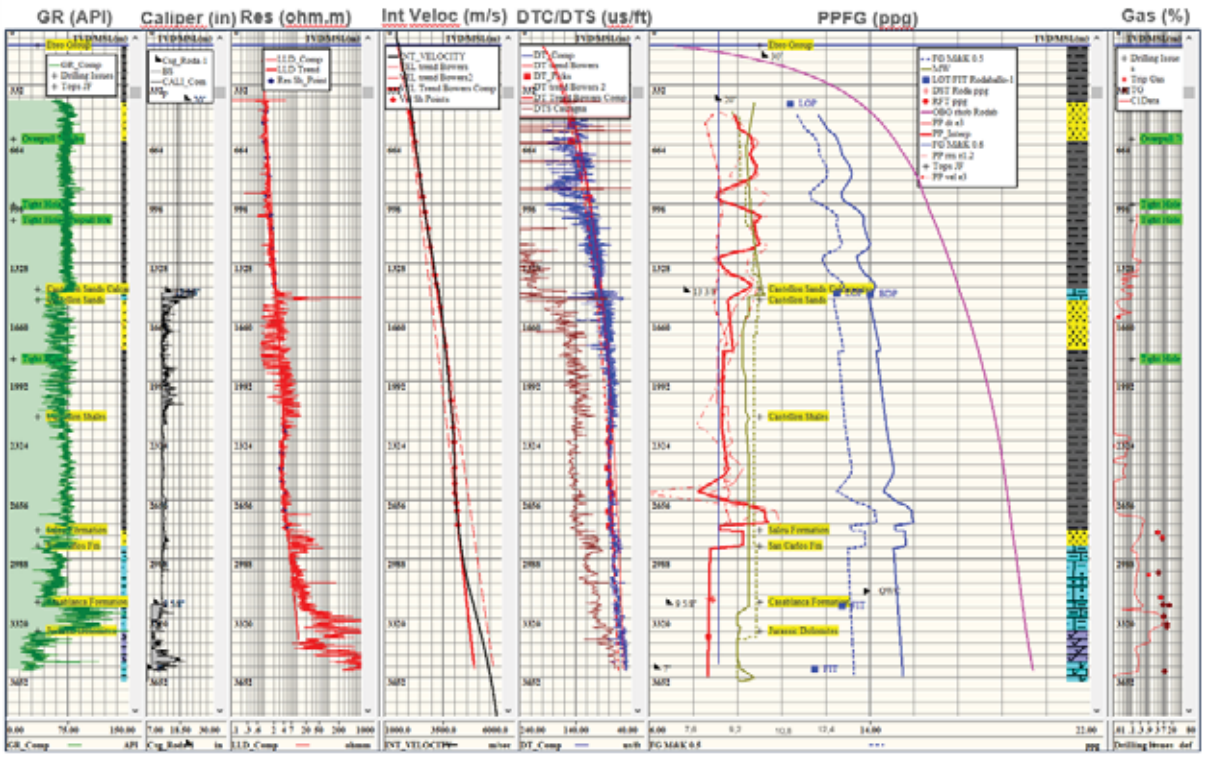

Figure 5-9 Input Data and Pore Pressure Fracture Gradient Prediction of Rodaballo-1 Well. Observe the two fracture gradients calculated based on LOT and FIT and the M&K relationship, considering two scenarios (0.5 dash blue line, conservative and 0.6 solid blue line, optimistic).

To calculate the Pore Pressure Fracture Gradient (PPFG) profiles we followed the next steps :.

1. **Overburden Profile using Density log**: Estimated through Miller formula from 700m to seabed, then used Density log from wireline (from 700 to 3650m).
2. To calculate the **Sonic normal compaction trend** (NCT) two trends are used:

   1- from seabed to Base Castellon Sands (Bowers method A:14.3 & B:0.775).

   2- from Castellon Shales to TD (Bowers method A:14.3 & B:0.745).

3. **Pore pressure calculation** (Eaton's formula) from Sonic and resistivity logs

Pore pressure is a maximum in the Ebro Fm. (10 ppg = pounds per gallon) with no evidence of underbalanced drilling (mud weight less than the formation pressure), A 9 ppg aquifer gradient is deduced from the mud weights used in the area. There was DST available in Casablanca Fm. (Limestones) showing a pressure of 8.6 ppg which supports this.

4. **Fracture gradients** (Mathew's & Kelly formula):

To calibrate the fracture gradients we collected 4 Leak Off Test results in each section of the well , presented as the mudweight in pounds per gallon which would give that pressure when extrapolated from the top of the well.

461 mMDRT:11.03 ppg (Ebro Fm.)

The PilotSTRATEGY project has received funding from the European Union's Horizon 2020 research and innovation programme under grant agreement No. 101022664

1523 mMDRT:12.8 ppg (Castellon Fm.)

3275 mMDRT: 13 ppg (San Carlos Fm.)

3630 mMDRT: 12 ppg (Mesozoic)

Finally the Fracture gradient profile was calculated based on the leak off test values.

Shmin = 0.45 x ESR M&K (worst case scenario honoring LOT Data).

Shmax = 0.6 x ESR M&K (assuming high regional fracture values).

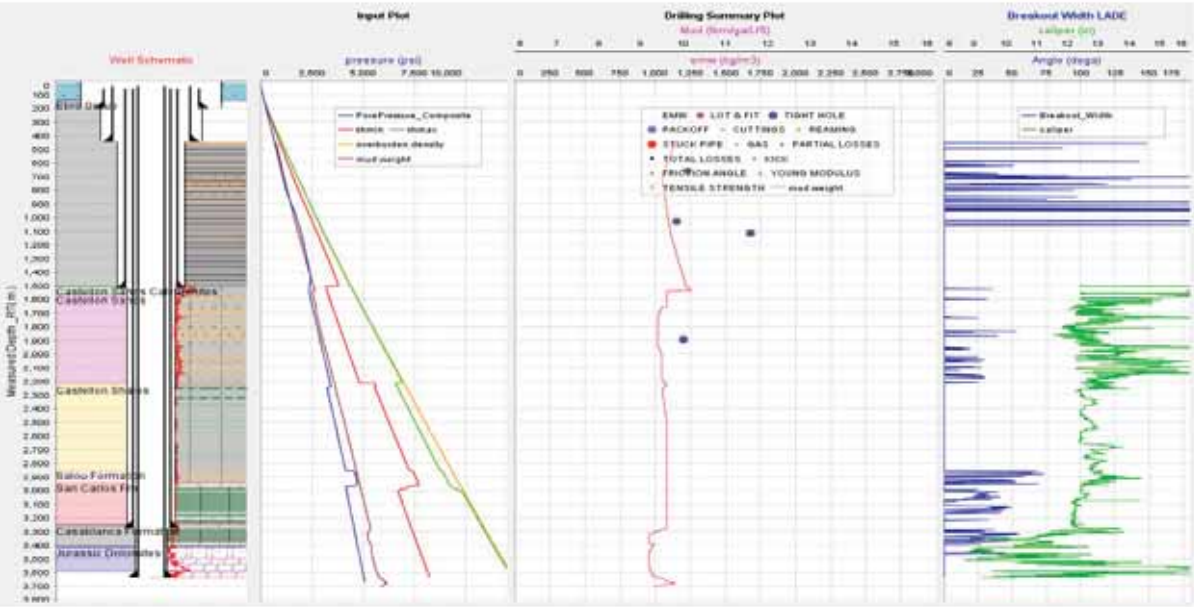

Figure 5-10 Elastic and geomechanical parameters calculated for Rodaballo-1 Well

Same corrections to McNally and Lal experimental relationship to calculate UCS have been performed in this well to calibrate the Caliper log with the Breakout Width.

The PilotSTRATEGY project has received funding from the European Union's Horizon 2020 research and innovation programme under grant agreement No. 101022664

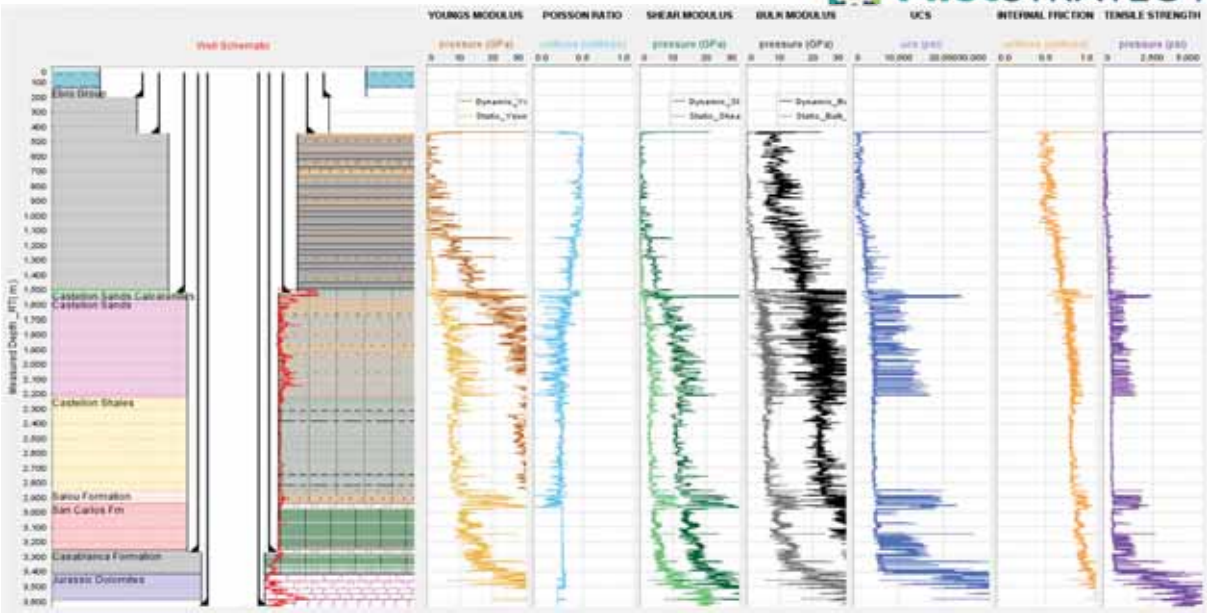

Figure 5-11 Well schematic, in-situ stress prediction, mudweight and breakout analysis to QC the model in Rodaballo-1 well

5.3.3 Sardina-1 Well

The sardina-1 well had a full set of logging data except for DTS available. As in the other wells, the Shear Sonic was estimated using Castagna relationships. The interval velocity available had a doubtful response. And no deviation survey data is available at the moment of this study so the well is assumed to be vertical.

The Upper Ebro Fm is characterized from seabed to 490mMDRT by a low GR response, possibly due to Ebro Fm being calcareous.

From 490m to 1650 mMDRT, the lower Ebro formation or Ebro shale is described as soft, plastic claystone, slightly to highly calcareous. There are fossil fragment present and the beds are mainly composed of siltstone and sandstones (fine to medium grained) lithologies.

From 1650mMDRT to 2570mMDT the Castellón sandstone is composed of interbedded sandstone and shales, slightly calcareous.

The only drill event registered was well below our formation of interest, in the Jurassic dolomites and it consisted of a stuck pipe event at 3900 mMDRT.

The PilotSTRATEGY project has received funding from the European Union's Horizon 2020 research and innovation programme under grant agreement No. 101022664

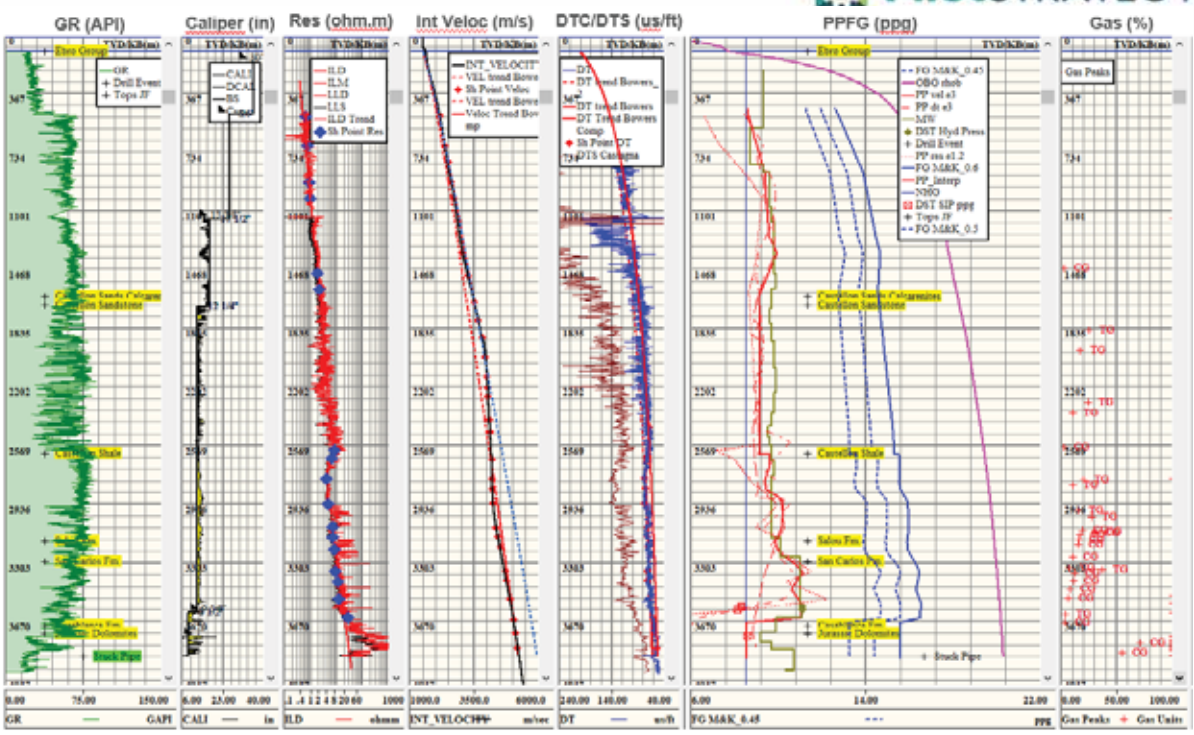

Figure 5-12 Input Logs and Pore Pressure Fracture Gradient Calculation for Sardina-1 well. The 0.45, 0.5, and 0.6 lines corresponds to scenarios for fracture gradient showing increasing operational window.

To calculate the Pore Pressure Facture Gradient profiles we have followed the next steps:

1. **Overburden Profile** using Density log for the missing section: Estimated through the Miller Formula from 500m to seabed.
2. **Sonic normal compaction trend NCT:**

   Two trends were used:

   Sonic and Interval Velocity NCT

   1- from seabed to base Castellon sands (Bowers method A:14.3 & B:0.775).

   2- from Castellon shales to TD (Bowers method A:14.3 & B:0.745).

3. **Pore pressure calculation** (Eaton's formula) from Sonic.

   Pore pressure with a maximum in the base of the Ebro Formation (10 ppg mudweight). It presents good caliper data, therefore, no there are no bad hole effects.

   Castellon Fm. reservoir pressure:

   Considered 9 ppg aquifer gradient from the mudweights used in the area.

   DST available in Casablanca Fm. at 8.6 ppg

4. **Fracture gradients (**Mathew's & Kelly formula) considering FIT results of

   486 mMDRT:11.5 ppg (Ebro Fm.)

The PilotSTRATEGY project has received funding from the European Union's Horizon 2020 research and innovation programme under grant agreement No. 101022664

3141 mMDRT:10.5 ppg (Casablanca Fm.)

Shmin = 0.4 x ESR M&K (worst case scenario assuming high calcareous content).

Shmax = 0.6 x ESR M&K (assuming high regional fracture values).

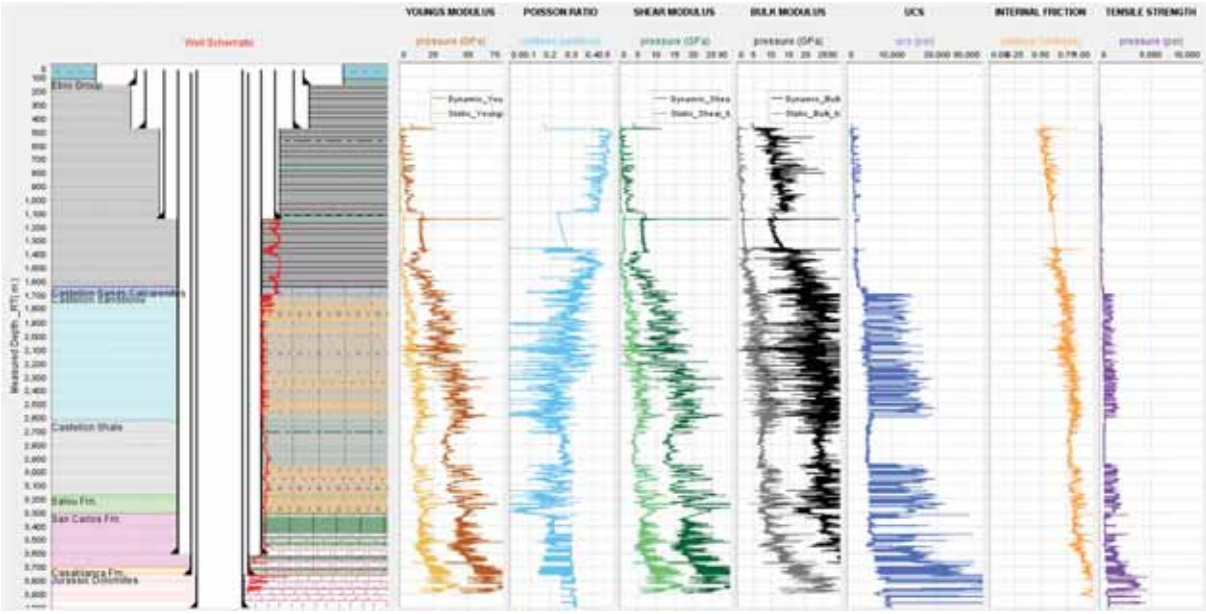

Figure 5-13 Elastic and geomechanical properties generated using the empirical relationship depicted in the text for the well Sardina-1

Same corrections to McNally and Lal experimental relationship to calculate UCS have been performed in this well to calibrate the Caliper log with the Breakout Width.

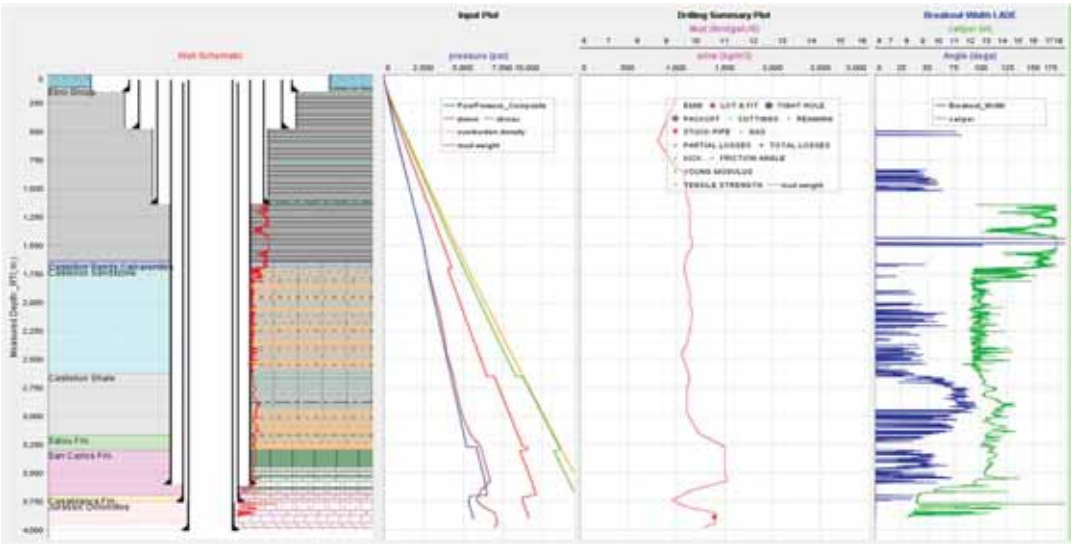

Figure 5-14 Well Schematics, in-situ stress, mudweight and breakout analysis for Sardina-1 well

The PilotSTRATEGY project has received funding from the European Union's Horizon 2020 research and innovation programme under grant agreement No. 101022664

5.3.4 Conclusions on in situ stresses calculation

In the absence of geomechanical analysis from the PilotSTRATEGY Project laboratories due to the absence of suitable sized rock samples, 3 wells were analyzed using experimental relationships. This work has allowed us to obtain elastic parameters that might be the best approximation with the data available to populate any future dynamic model in the area.

Rock density was estimated from different intervals and different wells using RHOB log and miller formula when absent. The overall values are very similar along the entire region.

Two different compaction trends were used due to the Messinian unconformity effect using different parameters or the Bower's method

- Ebro Fm.: (A:14.2 B:0.775)
- Castellon Shale-San Carlos Fm. (A:14.2 B:0.745)

The Pore pressure calculation was estimated using Eaton's method (exponent: 3) and Mathew's & Kelly formula for the fracture gradient (ESR:0.4 and 0.6).

In summary, for the two formations of interest, Ebro Formation (Upper Seal) and Castellon Formation (Reservoir) have been geomechanically described as follows:

Ebro Formation:

- The Ebro shale formation shows two different intervals:
  - 760-1110 mMD: Silty claystone characterized by "large scale foresets"
  - 1110-1560 mMD: Most uniform plastic claystone and some interbedded sandstone intervals, and some marls described.
- The rest of the wells present a single interval in the Ebro Fm. described as plastic poorly consolidated calcareous claystones with calcarenites and some sandstones stringers.
- Several drill events associated with bit balling and tight spots are associated with plastic behavior of the Ebro Shales.
- The pore pressure gradient is clearly hydrostatic with a possible slight increase at the base of the Base Ebro Fm. to above mud weight values. No underbalanced events are detected at this depth, therefore, it could be a possible false pore pressure increase due to a sonic anomaly associated with a caliper value increase (i.e. an enlarged borehole diameter), high organic content (described in the masterlog), or other reason. In the case that the detected overpressure is real (as seen in several wells), the capacity of the top seal will be enhanced.
- For the Ebro formations fracture gradient prognosis, the most realistic estimate is between 0.6-0.7 times the Effective Stress Ratio.

Castellon Formation:

- Described as **interbedded sandstones with high calcareous content.**
- The **pore pressure was defined as 8.5 - 9.1 ppg** in all of the wells. The aquifer pressure was interpreted as hydrostatic (8.55 ppg) on the basis of the performed analyses.

The PilotSTRATEGY project has received funding from the European Union's Horizon 2020 research and innovation programme under grant agreement No. 101022664

- The LOT values taken in Castellon Fm. are associated to the upper portion of the unit, described as a calcarenite level. Therefore, **the fracture gradients in the formation are of 0.4-0.5 times the Effective Stress Ratio,** being clearly reduced due to the calcareous content. It could be enhanced if no calcareous content at the top of the formation is present.

Conclusions on 1D Geomechanical log estimations:

- Through the empirical and log analyses described above, we have predicted the mechanical and elastic properties of some of the key wells close to the objective structure. Analogue studies have been analyzed to compare the results and calibrations. However, hard data must be acquired and analyzed in the lab for correct predictions in a future pilot well.
- From the results of this study, a normal tectonic regime is interpreted (Sv>SH>Sh – meaning that the vertical stress is higher than the horizontal ones). However, according to regional studies Sv is close to SH in the AOI.
- The Castellon Formation shows a higher stress anisotropy between SH and Sv than the upper seal (Ebro Formation).
- The world stress map (Figure 5-15) suggests SH (max. horizontal stress) is orientated at 030º azimuth in the area. Due to the possible stress anisotropy, the azimuth represents an important input for further fault stress analyses and should be confirmed by well breakouts analysis.
- The low pore pressure, and the vertical stress calculation (from WL RHOB) suggest a high operational pressure window, so there is enough pressure available to inject the CO2 without fracturing the formation.
- Additional laboratory analysis of rock properties are needed to build a poro-elastic model which would confirm these first approach based on empirical relationships.

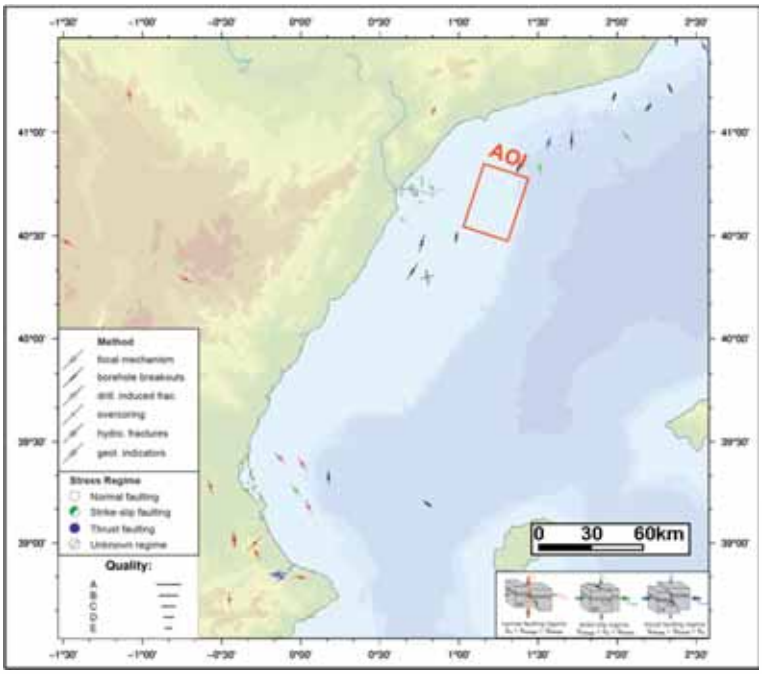

Figure 5-15 Regional World Stress Map showing SH orientation of 30°AZ

The PilotSTRATEGY project has received funding from the European Union's Horizon 2020 research and innovation programme under grant agreement No. 101022664

5.4 References

Bowers, G.L., 1995. Pore pressure estimation from velocity data: accounting for overpressure mechanisms besides undercompaction. SPE Drill. Complet. 89 (95).

Castagna et al., 1985. Relationships between compressional-wave and shear- wave velocities in elastic silicate rocks. Geophysics, 50 (4). P.11

Eaton, B.A., 1975. The Equation for Geopressure Prediction from Well Logs. SPE5544-MS.

Gardner, G.H.F., Gardner, L.W., Gregory, A.R., 1974. Formation velocity and density: the diagnostic basics for stratigraphic traps. Geophysics 39, 770 (780).

Golubev, A.A., Robinovich, G.Y., 1976. Resultaty primeneia appartury akusticeskogo karotasa dlja predeleina proconstych svoistv gormych porod na mestorosdeniaach tverdych isjopaemych. Prikl Geofiz Moskova 73, 109–116.

Lal, M. Shale stability: drilling fluid interaction and shale strength. paper SPE 54356, 1999.

Matthews WR, Kelly J. How to predict formation pressure and fracture gradient. Oil Gas J. 1967;65(8):92–106.

McNally, G. H. N. 1987. “Estimation of coal measures rock strength using sonic and neutron logs,” Geoexploration Vol. 24, pp 381–395.

Militzer, H., Stoll, R., 1973. Einige Beiträige der Geophysik zur primädatenerfassung im Bergbau: Neue Bergbautechnik. Leipzig 3, 21–25.

Miller, J. B. (1967). A formula for average foliage density. Aust. J. Bot. 15, 141-4.

Terzaghi, K., 1943. Theoretical Soil Mechanics. Wiley, New York.

Zoback, M. 2007. “Reservoir Geomechanics” New York: Cambridge University Press.

The PilotSTRATEGY project has received funding from the European Union’s Horizon 2020 research and innovation programme under grant agreement No. 101022664

6. Samples from Portugal

6.1 Geological aspects: overview

In the Lusitanian Basin two complexes with storage potential were previously identified: (i) Triassic-L Jurassic complex and (ii) Lower Cretaceous-Upper Cretaceous complex.

Triassic-Early Jurassic complex includes a caprock of Hettangian sediments (evaporites – halite and gypsum mainly – marls, dolomites, dolomitic limestones and claystone), overlying the Triassic siliciclastic reservoir.

The Cretaceous complex includes an Upper Cretaceous carbonate seal overlying a Lower Cretaceous siliciclastic formation. Most of the seal lithologies are compact limestones, with some sporadic interlayered marls and clays. The Lower Cretaceous reservoir consists of sandstones of variable grain sizes with some silt/clay layers interlayered. In some sectors of the Lusitanian Basin, the Upper Jurassic is also siliciclastic, and ca be included in the reservoir complex.

During the field work campaigns, all the lithologies of both storage complexes were sampled.

6.2 Samples from the onshore

To overcome the lack of core samples to be studied outcrop samples from both reservoir complexes were collected onshore. The sampling strategy was to obtain a set of samples representative of the lithological variability of the reservoirs and the seals. Not all the samples were suited to geomechanical analyses and a synthetic description of their mineralogical and textural characteristics are presented below in Table 6.1:

Table 6-1 - Studied Outcrop Samples

Sample	Age	Type	Observations
ARS-19	Triassic	Reserv.	Sandstone: mainly quartz grains; poorly calibrated; clast supported; abundant iron oxides/hydroxides. *XRD*: Quartz + K-feldspar ± Hematite
ARS-20	Triassic	Reserv.	Sandstone; quartz grains and lithoclasts; poorly calibrated; clast-supported; siliceous cement; iron oxides/hydroxides disseminated. *XRD*: Quartz + Orthoclase
ARS-22	Triassic	Reserv.	Sandstone; argillaceous cement. *XRD*: Quartz + K-feldspar + kaolinite
CC-CV-4	Triassic	Reserv.	Sandstone; sub-angular to subrounded grains; poorly calibrated; argillaceous cement. *XRD*: Quartz + K-feldspar + Kaolinite
PRVT-23	Triassic	Seal	Siltstone/claystone; abundant gypsum. *XRD*: Gypsum + K-felspar + Kaolinite + Dolomite ± Quartz ± Hematite
PPV-HT-28	Triassic	Seal	Fine grained sandstone; carbonate cement. *XRD*: Quartz + Calcite + Kaolinite ± Micas ± Microcline

The PilotSTRATEGY project has received funding from the European Union's Horizon 2020 research and innovation programme under grant agreement No. 101022664

RNA-16	Cretaceous	Seal	Wackstone; abundant bioclasts (gastropod and lamellibranchs); profusion of stylolites; *XRD*: Calcite
FR-SIB-26	Cretaceous	Seal	Dolomite, with some quartz and K-feldspar detrital grains and secondary calcite. *XRD*: Dolomite ± Calcite ± Quartz ± K-feldspar
CD-DARN-14	Cretaceous	Reserv.	Sandstone; fine grained; carbonate cement; quartz grains; poorly calibrated. *XRD*: Quartz + K-feldspar + Calcite
PAJ-29	Upper Jurassic	Reserv.	Sandstone; angular grains; carbonate cement; matrix-supported. *XRD*: Quartz + Orthoclase + Mg Calcite + Kaolinite

The PilotSTRATEGY project has received funding from the European Union's Horizon 2020 research and innovation programme under grant agreement No. 101022664

6.3 Well Data Availability

13 vertical wells were analysed in this study, 7 offshore and 5 onshore. The wells are mostly from the 70s (and some, the Monte-Real wells, from the 50s) with limited data acquisition and generally poor hole quality, which is illustrated through several wash-outs recorded in some of the most interesting formation targets. Figure 1 summarizes the available logs used in the interpretation.

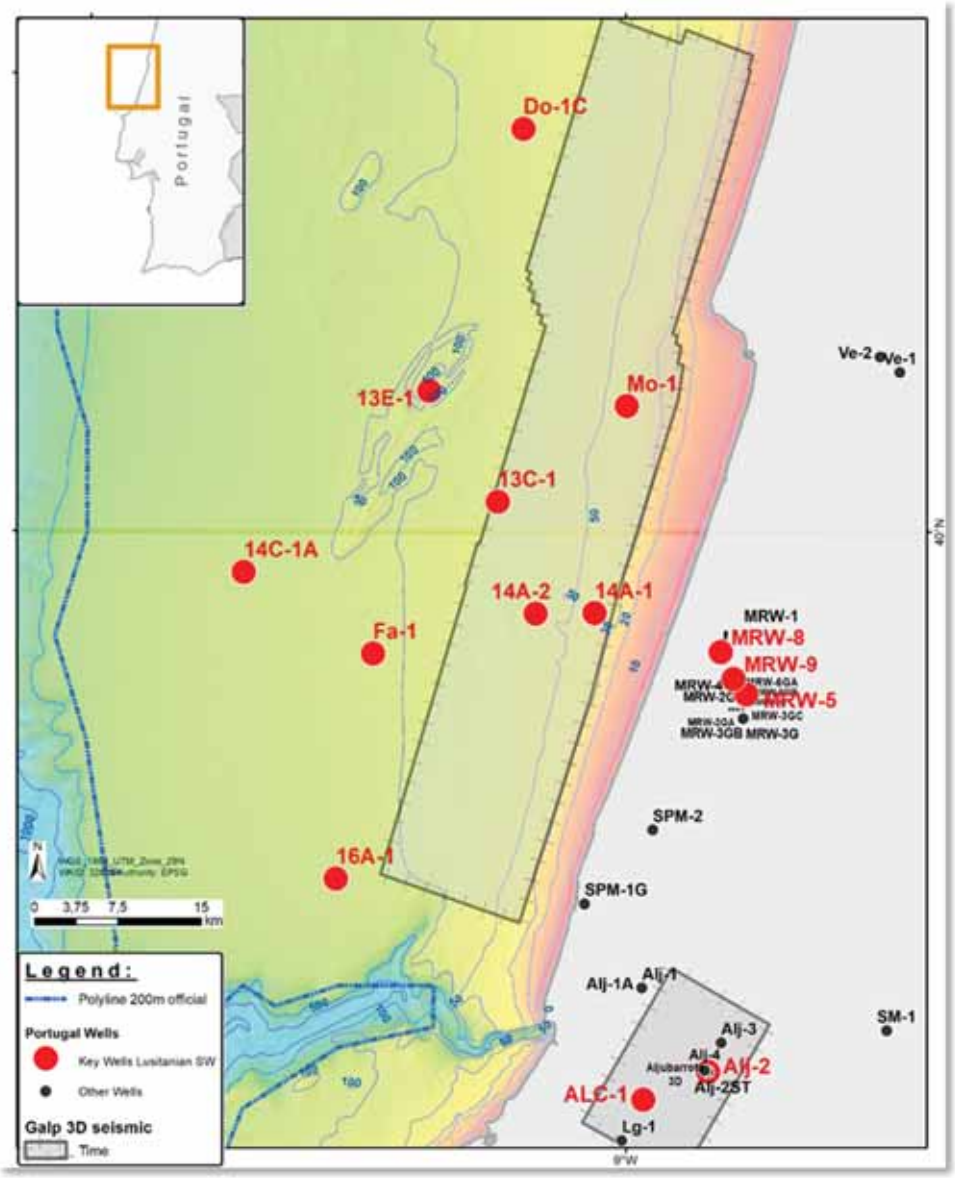

Figure 6-1 – Location map with the indication in red of the wells that were analyzed in this petrophysical study

Several washouts were identified based on Caliper logs, which influences the other log readings and increases the uncertainty in the geomechanical assessment.

Due to the vintage character of some of the wells drilled in different exploration campaigns, and without routine core analysis and dynamic tests, it was impossible to calibrate the calculated porosities with 100% certainty.

Table 6-2: WELL LOG DATA AVAILABILITY

	Well	Formation		Available Logs							
		Silves	Torres Vedras	Cal	GR	Spec GR	Den	Neu	Pef	Res	Dt
Offshore	Do-1C	x	x	x	x	-	x	x	-	x	x
	Mo-1	-	x	x	x	-	x	x	-	x	x
	13E-1	-	x	x	x	-	x	x	-	x	x
	13C-1	x	x	x	x	-	x	x	-	x	x
	14C-1A	-	x	x	x	-	x	x	-	x	x
	Fa-1	x	x	x	x	-	x	x	-	x	x
	16A-1	-	x	x	x	-	x	x	-	x	x
Onshore	Alc-1	x	-	x	x	x	x	x	x	x	x
	Alj-2	x	-	x	x	x	x	x	x	x	x
	MRW-5	-	-	-	x	-	-	x	-	x	-
	MRW-8	-	-	-	x	-	-	x	-	x	-
	MRW-9	-	-	-	x	-	-	-	-	x	-

6.4 Geomechanical results

6.4.1 Test adaptation

Geomechanical characterization of rock formations is usually done through standard laboratory tests. For the formations of the Lusitanian Basin (LB) selected as potential reservoirs and seals the lack of samples collected at a depth equivalent to the required depth for carbon storage is a constraint for the interpretation of the obtained results. Representative samples were collected at outcrops and tested for the required parameters. Some adaptation was needed to obtain the required mechanical parameters due to the constrains on the available laboratorial equipment.

The set of parameters included in the initial work plan were:

Uniaxial Compressive Strength (UCS);

Tensile Strength (BST);

Elasticity Modulus (E);

Static Elastic Modulus;

The PilotSTRATEGY project has received funding from the European Union's Horizon 2020 research and innovation programme under grant agreement No. 101022664

Dynamic Elastic Modulus.

The tests used to determine these parameters were:

1. P-wave propagation velocity

Dynamic Elasticity modulus (Ed) can be estimated from the p-wave velocity (Vp) and density values of the studied materials. Ed values are generally slightly higher than the values of the Elasticity Modulus (E).

Vp determination was done using a PUNDICT equipment, according to the protocol described in the British Standard BS 1881 Part 203. Poisson Coefficient values (n) used in the calculation were determined using the Equation 1 (Vallejo et al., 2002).

$$n = \frac{\left(V_p/V_s\right)^2 - 2}{2\left[\left(V_p/V_s\right) - 1\right]}$$

where Vp and Vs are the propagation velocities of the p-waves and the s-waves.

For each sample 7 5 cm x 5 cm x 5 cm cubes were tested along the 3 possible directions. The existence of anisotropies parallels to the faces of the cube implied differences in the determined values of Ed.

The results of P-wave propagation velocity are presented in Table 6-3.

2. Point Load Strength Index Test

Geomechanical parameters such as Tensile Strength (BTS), Uniaxial Compressive Strength (UCS) and Elasticity Modulus (E) can be estimated from the point load test, using correlation equations found in the literature.

The test was done in using samples with a square base of 5 cm x 5 cm and 10 cm height. With this geometry there is no need to introduce a correction factor whereby Is = Is(50). The number of test pieces ranged between 5 and 7. The standard used for the point load determination was ASTM D 5731-95.

Results of the estimates from the point load strength index are presented in the following tables: BTS (Table 6-4), UCS (Table 6-5) and E (Table 6-6), for the sampled lithologies.

3. Determination of Uniaxial Compressive Strength using the Schmidt Hammer

A Schmidt Hammer allows the determination of the material's resistance to the impact of the hammer shoot (rebound resistance). This parameter in conjunction with the sample density can be used to graphically estimate the UCS. Also several numerical expressions account for the correlation between the rebound resistance and UCS, for different lithological materials. This study applied the equations for the same lithologies as the reservoir and seal of the Lucitania Basin. Table 6-7 presents the obtained results.

Elasticity Modulus (E) was also calculated from the Schmidt Hammer test, using the numerical approaches from published papers and the results are presented in Table 6-8.

The PilotSTRATEGY project has received funding from the European Union's Horizon 2020 research and innovation programme under grant agreement No. 101022664

6.4.2 Geomechanical measurements: results

Table 6-3 - Dynamic Elasticity Modulus (Ed)

Parameter	Dynamic Elasticity Modulus (Ed)					
Test	P-wave propagation speed - ϑ					
Correlation	$Ed = \rho * \vartheta^2 * \left[\frac{(1+\vartheta)*(1-2\vartheta)}{(1-\vartheta)}\right]$					
Measurement direction	NA		Parallel to anisotropy		Perpendicular to anisotropy	
Sample	Average (GPa)	Stan. Dev.	Average (GPa)	Stan. Dev.	Average (GPa)	Stan. Dev.
ARS-19	19,51	2,89				
RNA-16	2,55	0,03				
FR-SIB-26	14,51	2,76				
ARS-22	16,01	2,06	17,01	1,42	11,31	1,13
PAJ-29	25,93	3,98	29,29	4,29	16,79	2,71

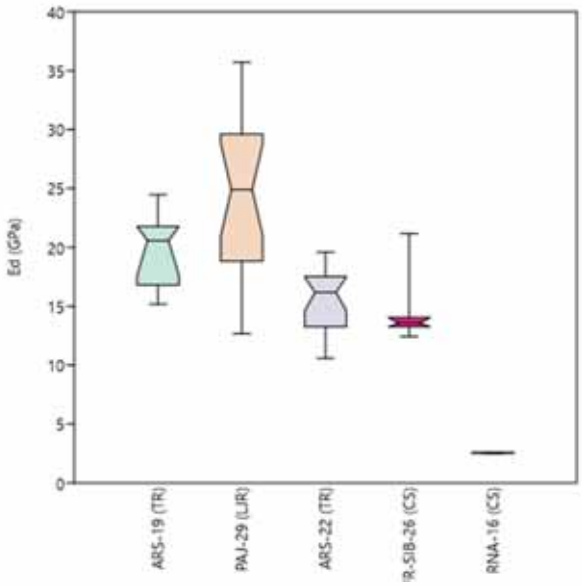

Figure 6-2 – Dynamic elasticity module. (TR: Triassic Reservoir; LJR: Lower Jurassic Reservoir; CS: Cretaceous seal)

The PilotSTRATEGY project has received funding from the European Union's Horizon 2020 research and innovation programme under grant agreement No. 101022664

Table 6-4 - Tensile Strength from Point Load (BTS)

Parameter	Tensile Strength (BTS)	
Test	Point Load	
Correlation	$BTS = Is_{(50)} * 0.67$	
Sample	Average (MPa)	Stan. Dev.
ARS-19	0.41	0.13
RNA-16	1.08	0.46
FR-SIB-26	0.38	0.10
ARS-22	1.04	0.14
PAJ-29	0.32	0.08

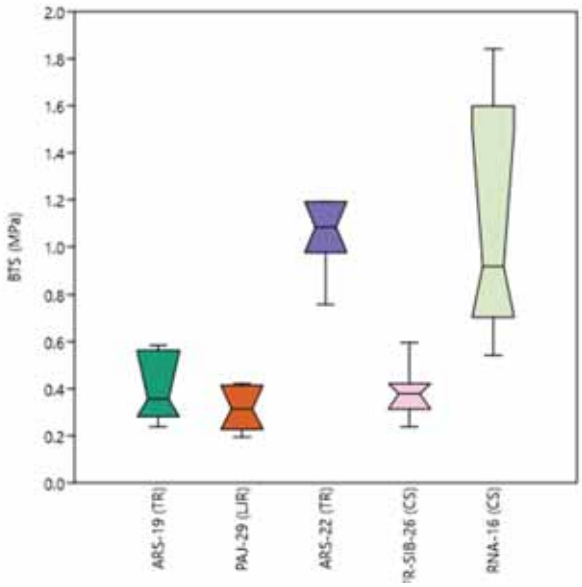

Figure 6-3 -Tensile strength estimated from point load test. (TR: Triassic Reservoir; LJR: Lower Jurassic Reservoir; CS: Cretaceous seal)

The PilotSTRATEGY project has received funding from the European Union's Horizon 2020 research and innovation programme under grant agreement No. 101022664

Table 6-5 - Uniaxial Compressive Strength from Point Load (UCS)

Parameter	Uniaxial Compressive Strength (UCS)	
Test	Point Load	
Correlation	$UCS = 17.57 * Is^{1.1555}$	
Sample	Average (GPa)	Stan. Dev.
ARS-19	9.71	3.59
RNA-16	30.05	14.65
FR-SIB-26	8.86	2.83
ARS-22	28.17	4.35
PAJ-29	7.17	2.18

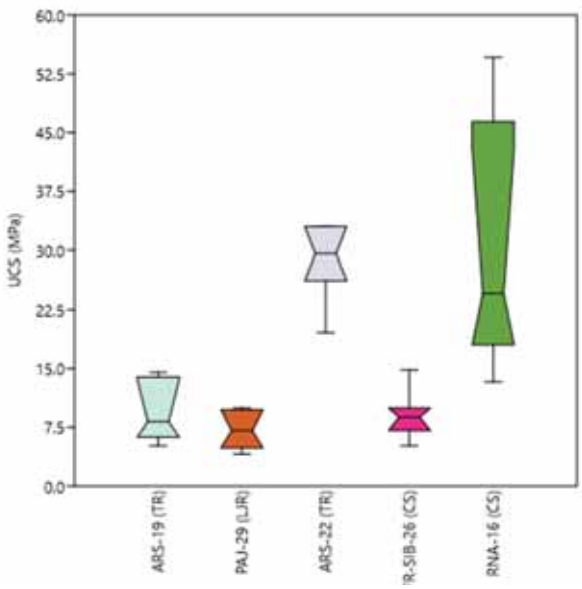

Figure 6-4 – Uniaxial compressive strength estimated from point load test. (TR: Triassic Reservoir; LJR: Lower Jurassic Reservoir; CS: Cretaceous seal)

The PilotSTRATEGY project has received funding from the European Union's Horizon 2020 research and innovation programme under grant agreement No. 101022664

Table 6-6 - Elasticity Modulus from Point Load(E)

Parameter	Elasticity Modulus (E)	
Test	Point Load	
Correlation	$E = 11.409 * Is^{0.9322}$	
Sample	Average V. (GPa)	Stan. Dev.
ARS-19	6.99	2.11
RNA-16	17.28	6.85
FR-SIB-26	6.51	1.66
ARS-22	16.67	2.11
PAJ-29	5.50	1.36

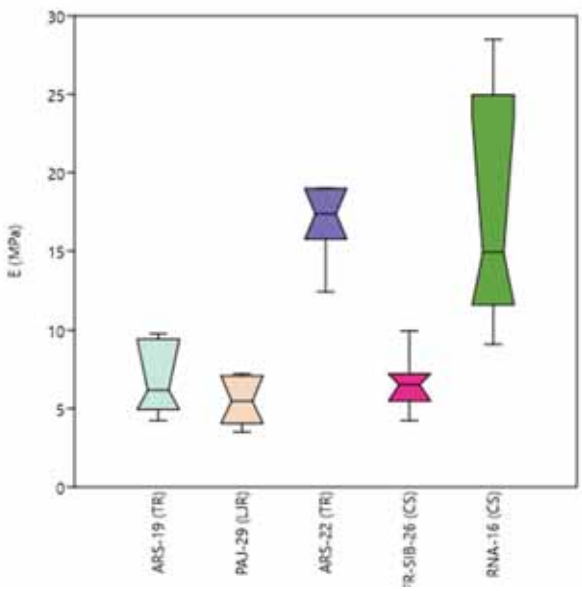

Figure 6-5 – Elastic modulus estimated from point load test. (TR: Triassic Reservoir; LJR: Lower Jurassic Reservoir; CS: Cretaceous seal)

The PilotSTRATEGY project has received funding from the European Union's Horizon 2020 research and innovation programme under grant agreement No. 101022664

Table 6-7 -Uniaxial Compressive Strength from Schmidt Hammer (UCS)

Parameter	Uniaxial Compressive Strength (UCS)			
Test	Schmidt Hammer			
Correlation	Direct		$UCS = 2.208 * e^{0.067*R}$	
Sample	Average (MPa)	Stan. Dev.	Average (MPa)	Stan. Dev.
RNA-16	49.60	26.33	65.48	19.42
FR-SIB-26	24.73	1.61	49.70	3.03
ARS-22	30.93	3.91	61.86	6.85
PAJ-29	56.13	8.66	90.66	9.63
ARS-20	23.00	3.03	40.92	5.89
CC-CV-4	24.07	2.17	42.97	4.33
CD-DARN-14	69.60	7.00	100.11	4.78

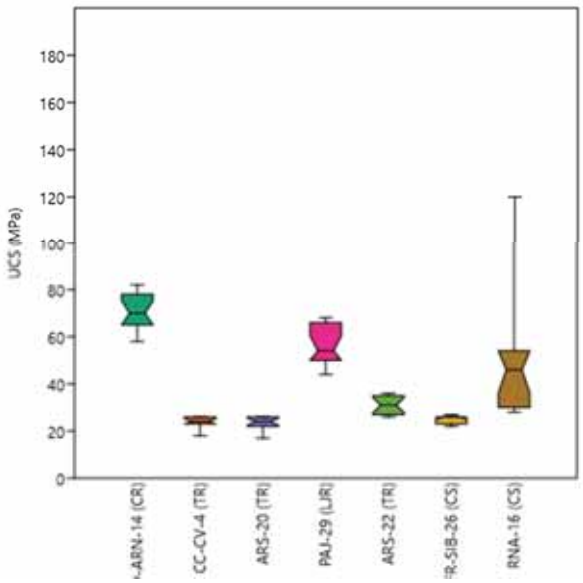

Figure 6-6 -Uniaxial compressive strength direct from Schmidt hammer. (TR: Triassic Reservoir; LJR: Lower Jurassic Reservoir; CS: Cretaceous seal)

The PilotSTRATEGY project has received funding from the European Union's Horizon 2020 research and innovation programme under grant agreement No. 101022664

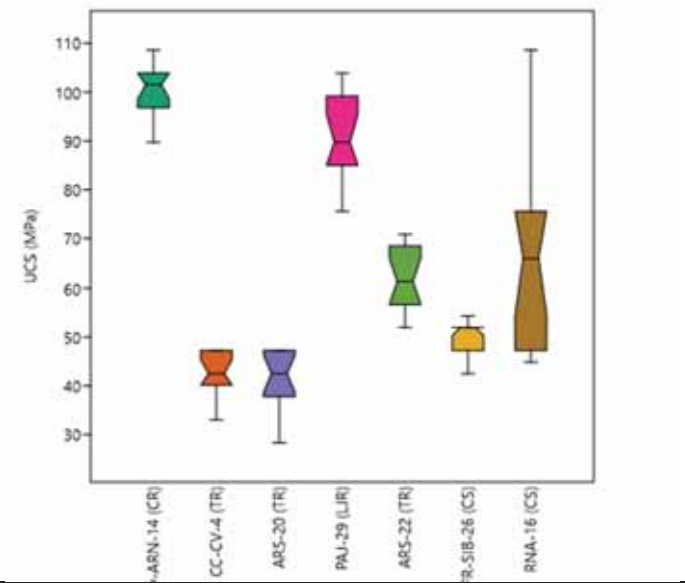

Figure 6-7 -Uniaxial compressive strength estimated from Schmidt hammer rebound values. (TR: Triassic Reservoir; LJR: Lower Jurassic Reservoir; CS: Cretaceous seal)

Table 6-8 - Elastic Modulus from Schmidt Hammer (E)

Parameter	**Elasticity Modulus (E)**	
Test	**Schmidt Hammer**	
Correlation	$E = 6.95 * g^2 * R - 1.14 * 106 * 10^{-3}$	
Sample	**Average (GPa)**	**Stan. Dev.**
ARS-19		
RNA-16	131.05	38.91
FR-SIB-26	59.75	3.65
ARS-22	83.26	9.24
PAJ-29	124.75	13.26
ARS-20	60.86	8.78
CC-CV-4	63.90	6.45
CD-DARN-14	149.04	7.13

The PilotSTRATEGY project has received funding from the European Union's Horizon 2020 research and innovation programme under grant agreement No. 101022664

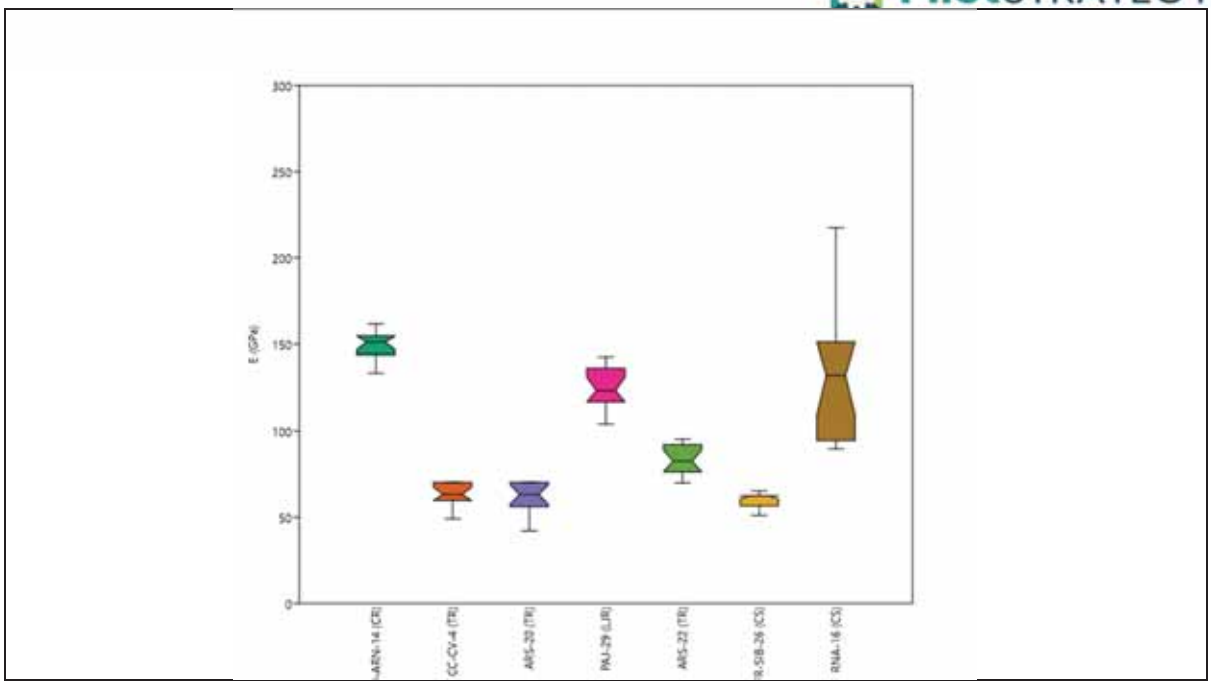

Figure 6-8 – Elastic modulus estimated from Schmidt hammer rebound. (TR: Triassic Reservoir; LJR: Lower Jurassic Reservoir; CS: Cretaceous seal).

6.5 References

[1] Alshkane, Y. M., & Hama Saeed, S. B. (2018). Effect of freezing and thawing on physical and mechanical properties of sedimentary rock. Journal of Garmian University, 5(2), 126-140.

[2] ASTM D 5731 – 95 - Standard Test Method for Determination of the Point Load Strength Index of Rock

[3] BS 1881 Part 203: Recommendations for measurement of velocity of ultrasonic pulses in concrete.1986

[4] Daoud, H. S. D., Rashed, K. A. R., & Alshkane, Y. M. A. (2017). Correlations of uniaxial compressive strength and modulus of elasticity with point load strength index, pulse velocity and dry density of limestone and sandstone rocks in Sulaimani Governorate, Kurdistan Region, Iraq. Journal of Zankoy Sulaimani, 19, 57-72.

[5] Deere, D. U., & Miller, R. P. (1966). Engineering classification and index properties for intact rock. Illinois Univ At Urbana Dept Of Civil Engineering.

[6] González de Vallejo, L. I., Ferrer, M., Ortuño, L., & Oteo, C. (2002). Ingeniería geológica. Pearson Educación.

[7] Katz, O., Reches, Z., & Roegiers, J. C. (2000). Evaluation of mechanical rock properties using a Schmidt Hammer. International Journal of rock mechanics and mining sciences, 37(4), 723-728.

[8] O'Rourke, J. E. (1989). Rock index properties for geoengineering in underground development. Min. Eng. (Littleton, Colo.);(United States), 41(2).

[9] Saleh Daoud, H., M Alshkane, Y., & Ahmad Rashed, K. (2018). Prediction of Uniaxial Compressive Strength and Modulus of Elasticity for Some Sedimentary Rocks in Kurdistan Region-Iraq using Schmidt Hammer. Kirkuk University Journal-Scientific Studies, 13(1), 52-67.

[10] Saptono, S., Kramadibrata, S., & Sulistianto, B. (2013). Using the Schmidt hammer on rock mass characteristic in sedimentary rock at Tutupan coal mine. Procedia Earth and Planetary Science, 6, 390-395.

[11] Singh, R., Hassani, F. P., & Elkington, P. A. S. (1983, June). The application of strength and deformation index testing to the stability assessment of coal measures excavations. In The 24th US Symposium on Rock Mechanics (USRMS). OnePetro.

[12] Yagiz, S. (2013). Comment on “Point Load Test on Meta-Sedimentary Rocks and Correlation to UCS and BTS” by Diyuan Li and Lous Ngai Yuen Wong, Rock Mechanics and Rock Engineering. Rock mechanics and rock engineering, 46(4), 909-912.

The PilotSTRATEGY project has received funding from the European Union’s Horizon 2020 research and innovation programme under grant agreement No. 101022664

7. Samples from Greece

7.1 Geological aspects

The Mesohellenic basin has a 150 km length and 30 km width. It is partly located in Northern Greece and partly in Albania and was developed from Middle Eocene to Upper Miocene. The Grevena sub-basin area has shown preliminary potential for CO_2 storage [Koukouzas et al, 2021].

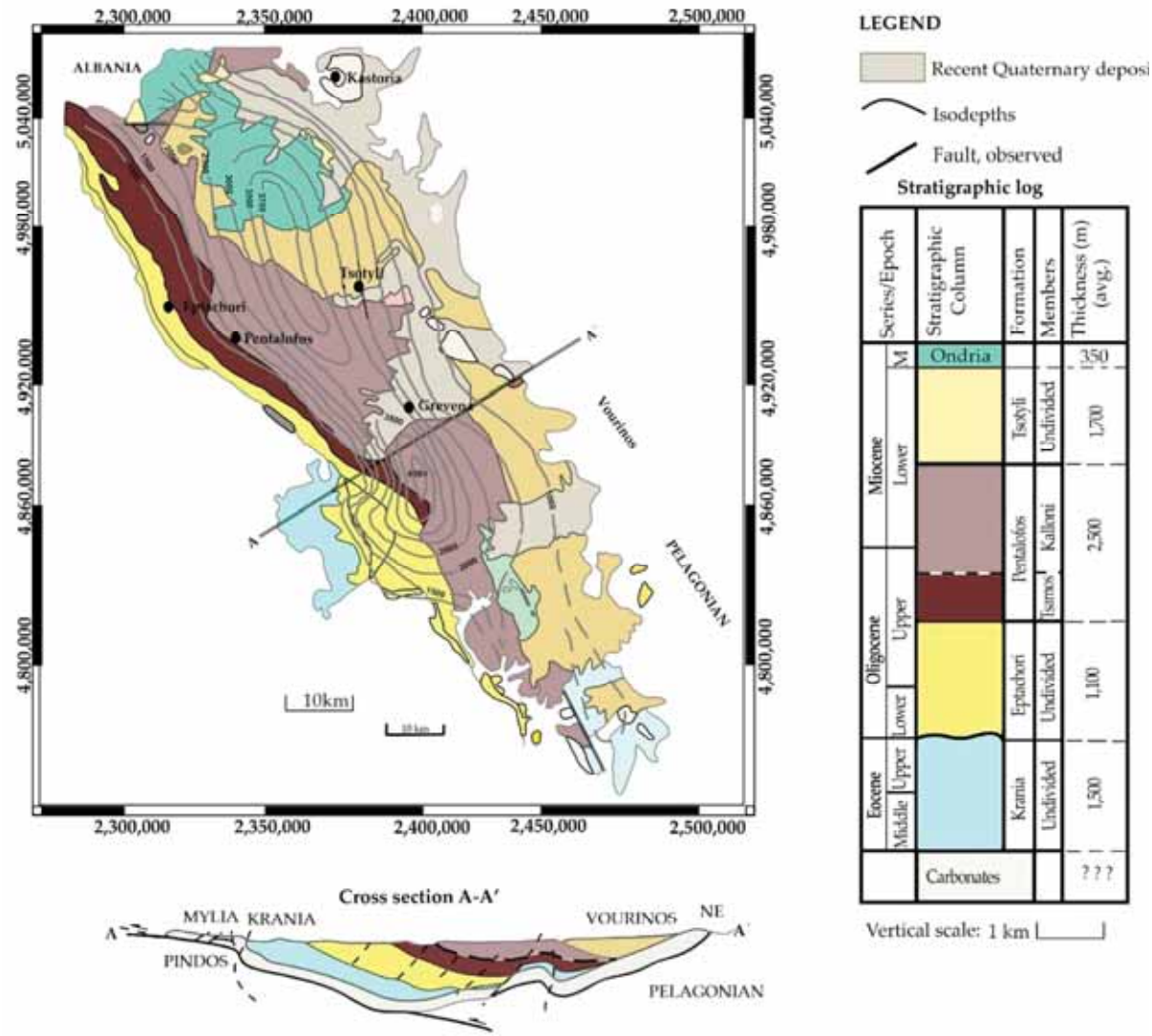

Figure 7-1.: Geological Map and stratigraphic column adapted from Ferriere et al., 2004, of the proposed CO2 Storage basins in Grevena area depicting Pentalofos and Eptachori formations, scale 1:1,000,000. Cross-sections of the Mesohellenic Trough. Lithological formations: Krania Turbidites, Eptachori, Taliaros, Pentalofos, Tsotyli. M stands for Middle Miocene, scale 1:500,000

During previous research three formations have identified with interest for further potential research related to CO2 storage. From top downwards, these are:

The PilotSTRATEGY project has received funding from the European Union's Horizon 2020 research and innovation programme under grant agreement No. 101022664

Tsotyli Formation. Alternation between units of varying grain size and strength:

1. 0.5-1.5m-thick beds of medium weak to very strong, partially weathered, grey conglomerate. Clasts are poorly sorted (0.5-10+mm with occasional larger clasts), sub-angular to sub-rounded, predominantly limestone with igneous/metamorphic clasts and fossil corals, grain-supported with clastic matrix. No interior bedding or structures. 2. 10cm-1m-thick beds of medium weak to very strong, partially weathered, gray greywacke. Grains are fine, angular, limestone-quartz-micas-various mafics.

Pentalofos Formation. Slightly weak to medium strong beds of partially weathered, grey sandstone. Grains are fine, crystalline, most are indistinguishable from matrix. Many mica and mafic grains. Sample effervesces in acid—either a calcareous matrix, or grains of limestone (could not be determined macroscopically). Some weak interior bedding. Occasional trace fossils (burrow casts). Iron oxide staining.

Eptachori Formation. Very strong, thickly bedded (20-30cm), partially weathered, medium grey-tan, fine greywacke. Joint fractures spaced 40-80cm apart, perpendicular to bedding. Trace fossils (invertebrate burrows) on bedding surfaces. Partially carbonized wood and leaf fragments. Water discoloration (Liesegang) penetrates 8-10cm into bedding.

From December 2021 to May 2023 several walk-over surveys were conducted to gather an initial set of data. During these surveys several field samples were collected from the Tsotyli, Pentalofos and Eptechori formation were collected and subsequently were sent to various laboratories for petrophysical and geomechanical investigation (Figure 7-2).

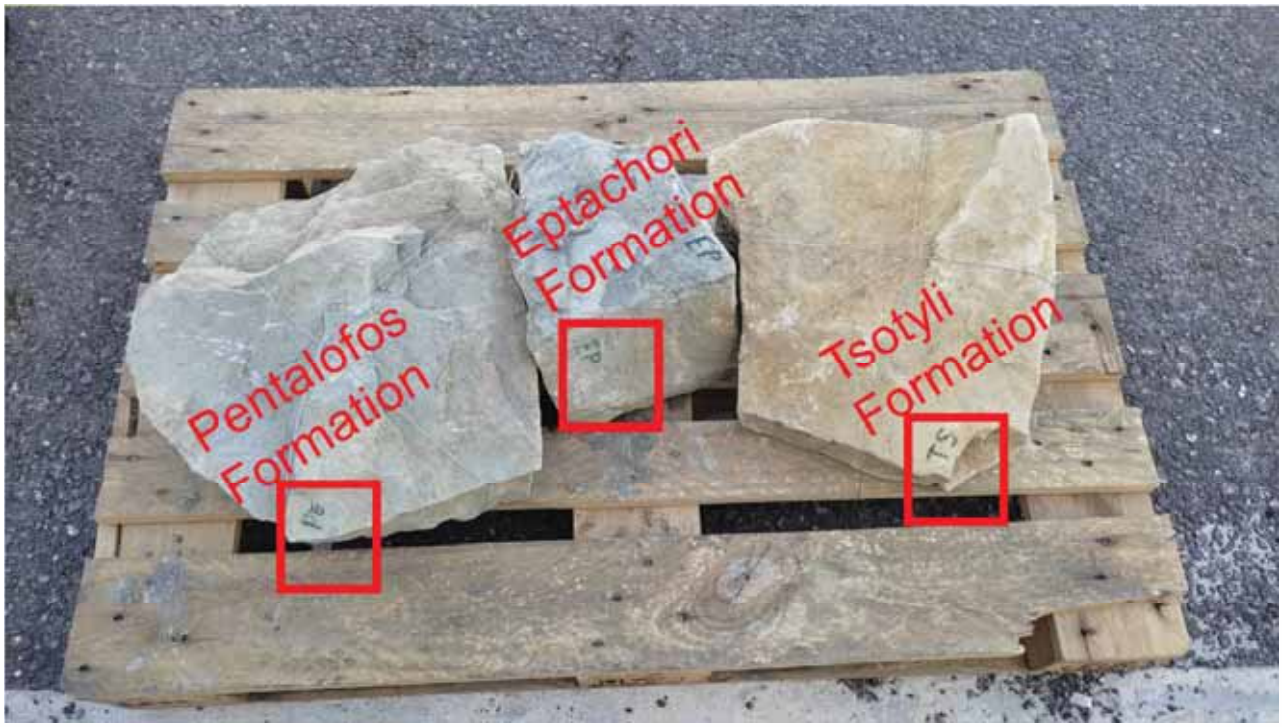

Figure 7-2.: Bulk samples collected during the initial walk over survey and sent to France: IFP Energies nouvelles – Earth Sciences and Environmental Technologies, Scotland: School of

The PilotSTRATEGY project has received funding from the European Union's Horizon 2020 research and innovation programme under grant agreement No. 101022664

CERTH is committed to open data and metadata sharing sample information in an effort to promote a workplace of collaboration. Therefore, data from the samples collected are open and accessible as follows:

Tsotyli formation https://app.geosamples.org/sample/igsn/IE5770001

Pentalofos formation https://app.geosamples.org/sample/igsn/IE5770002

Eptachori formation (https://app.geosamples.org/sample/igsn/IE5770003)

The PilotSTRATEGY project has received funding from the European Union's Horizon 2020 research and innovation programme under grant agreement No. 101022664

7.2 Geomechanical Characterisation

Geomechanical characterization of the Tsotyli (TS), Pentalofios (PE) and Eptachori (EP) formations was conducted through standard laboratory tests. Representative samples were collected (see section 7.1) at outcrops and tested for the required parameters. Some adaptation was needed to obtain the required mechanical parameters due to the constrains on the available laboratory equipment.

The initial proposed set of mechanical tests/parameters included were:

- Uniaxial Compressive Strength (UCS) – obtained through the Uniaxial compression test
- Tensile Strength (BST) - obtained through the Brazilian test
- Elasticity Modulus
    - Static Elastic Modulus – Uniaxial test (E)
    - Dynamic Elastic Modulus – Ultrasonic Velocity Measurements (Ed)

However due to the unavailability of some apparatus in the laboratory facilities some of the tests were replaced and the estimation of the mechanical parameters was done indirectly using other tests and application of published correlations.

Dynamic Elasticity Modulus (Ed) can be estimated from the p-wave velocity (Vp) and density values of the studied materials.

Vp determination was done using a PUNDICT equipment, according to the protocol described in the British Standard BS 1881 Part 203. Poisson Coefficient values (ν) used in the calculation were determined using the Equation 1 (Vallejo et al., 2002), where Vp and Vs are the propagation velocities of the p-waves and the s-waves.

Equation 1

$$n = \frac{\left(V_p/V_s\right)^2 - 2}{2\left[\left(V_p/V_s\right) - 1\right]}$$

For each sample seven cubes (5cm × 5cm × 5cm) were tested along the 3 possible directions. The results are presented in **Table 7-1**. All results below have been corrected to present data to two significant figures, therefore it differs slightly from the raw data received from the laboratory.

Table 7-1.: Dynamic Elasticity modulus (Ed) for Tsotyli (TS), Pentalofo (PT), Eptachori (EP).

Parameter	**Dynamic Elasticity modulus (Ed)**	
Test	**P-wave propagation speed - Vp**	
Correlation	**C1 - Ed**	
Sample	**Average V. (GPa)**	**Standard deviation**
TS	2,5	0,05
PE	38	2,8

The PilotSTRATEGY project has received funding from the European Union's Horizon 2020 research and innovation programme under grant agreement No. 101022664

EP	26	1,1

Geomechanical parameters such as Tensile Strength (BTS), Uniaxial Compressive Strength (UCS) and Elasticity Modulus (E) can be estimated from the point load test, using correlation equations found in the literature.

The test was done in seven samples with a square base with 5cm x 5cm and 10cm height. With this geometry there is no need to introduce a correction factor whereby Is = Is(50). The standard used for the point load determination was ASTM D 5731-95.

The determined values of Point Load Strength Index for the studied sampled and the estimated values of BTS are given in Table 7-2.

Table 7-2.: Tensile Strength (BTS) for Tsotyli (TS), Pentalofo (PT), Eptachori (EP).

Parameter	**Tensile Strength (BTS)**							
Test	**Point Load**							
Correlation	**C1 - BTS**		**C2 - BTS**		**C3 - BTS**		**C4 - BTS**	
Sample	**Average V. (MPa)**	**Standard deviation**	**Average V. (MPa)**	**Standard deviation**	**Average V. (MPa)**	**Standard deviation**	**Average V. (MPa)**	**Standard deviation**
TS	1,1	0,069	1,5	0,10	0,84	0,06	1,1	0,072
EP	1,6	0,17	2,8	0,28	1,3	0,15	1,6	0,20
PE	2,8	0,21	4,3	0,41	2,4	0,23	3,1	0,29

The determined values of UCS are given in Table 7.8.

Table 7-3.: Uniaxial Compressive Strength (UCS) for Tsotyli (TS), Pentalofo (PT), Eptachori (EP).

Parameter	**Uniaxial Compressive Strength (UCS)**	
Test	**Point Load**	
Correlation	**C5 - UCS**	
Sample	**Average V. (GPa)**	**Standard deviation**
TS	22	1,6

The PilotSTRATEGY project has received funding from the European Union's Horizon 2020 research and innovation programme under grant agreement No. 101022664

EP	35	5,0
PE	74	8,0

The Elastic modulus and E results are presented in the table**Table 7-4**:

Table 7-4.: Elasticity Modulus (E) derived from point load for Tsotyli (TS), Pentalofo (PT), Eptachori (EP).

Parameter	**Elasticity Modulus (E)**	
Test	**Point Load**	
Correlation	**C3 - E**	
Sample	**Average V. (GPa)**	**Standard deviation**
TS	14	0,84
EP	20	2,3
PE	36	3,2

The Schmidt Hammer test allows the determination of the material's resistance to the impact of the hammer (the rebound resistance). This parameter in conjunction with the sample density can be used to estimate the Uniaxial Compressive Strength (UCS), by using published numerical correlation between the rebound resistance and UCS. Results are presented in **Table 7-5**.

Table 7-5.: Uniaxial Compressive Strength (UCS**)** for Tsotyli (TS), Pentalofo (PT), Eptachori (EP).

Parameter	**Uniaxial Compressive Strength (UCS)**									
Test	**Schmidt Hammer**									
Correlation	**Direct**		**C1 - UCS**		**C2 - UCS**		**C3 - UCS**		**C4 - UCS**	
Sample	**Average V. (MPa)**	**Standard deviation**	**Average V. (MPa)**	**Standard deviation**	**Average V. (MPa)**	**Standard deviation**	**Average V. (MPa)**	**Standard deviation**	**Average V. (MPa)**	**Standard deviation**
TS	31	4,5	15	6,4	43	5,0	51	6,0	28	1
EP	35	3,5	61	19	61	4,7	71	5,6	71	12
PE	56	7,04	188	56	79	5,8	94	6,8	116	14

The PilotSTRATEGY project has received funding from the European Union's Horizon 2020 research and innovation programme under grant agreement No. 101022664

The Schmidt Hammer test also can be used to calculate the Elasticity Modulus (E), using numerical approaches from published papers. Results are presented in Table 7-6.

Table 7-6.: Elasticity Modulus (E) derived from Schmidt Hammer for Tsotyli (TS), Pentalofo (PT), Eptachori (EP).

Parameter	Elasticity Modulus (E)			
Test	Schmidt Hammer			
Correlation	C1 - E		C2 - E	
Sample	Average V. (GPa)	Standard deviation	Average V. (GPa)	Standard deviation
TS	95	11	10	3,4
EP	86	6,8	30	7,4
PE	126	9,2	72	17

7.3 Interpretation of results

The samples collected during the walk-over survey are indicative and represent the first attempt to understand the potential conditions in the area. However, they have been collected randomly and are neither based on a statistical sampling framework nor a focused survey. Thus, the results are not statistically representative of the area and any analysis must be interpreted with caution. Furthermore, the formations of Tsotyli, Pentalofos and Eptachori are divided into members and groups. Each one of them has different properties due to different sedimentary geological history. However, some helpful interpretations can be drawn to drive further investigation and research of the area.

Poisson's ratio, Young's modulus and Brittleness Index are used in the oil and gas industry by reservoir engineers for assessing the "frackability" of a source rock, as well as in injectivity of CO_2 in saline aquifers and depleted oil/gas fields. In view of the petrophysics results (PilotSTRATEGY deliverable D2.6), the geomechanical data should be seen as an upper boundary condition on the transboundary (contact) zone between the reservoir host rock and the cap layer rocks.

Results for the Youngs modulus derived from P-wave propagation speed (Dynamic Elasticity modulus) and the Point load test are in relatively close agreement apart from the Tsotyli formation. The latter disagreement could be the result of particular samples or the result of inelastic effects (Ciccotti et al., 2004). However, it should be noted that Dynamic Elasticity modulus is a measure of the stiffness of the rock mass when it is subjected to dynamic (or rapidly changing loads), such as in the case of an earthquake or the case of vibrating structures or moving machinery. Elasticity modulus, on the other hand, is a measure of stiffness under static or constant loading. Therefore, it is expected that Dynamic

The PilotSTRATEGY project has received funding from the European Union's Horizon 2020 research and innovation programme under grant agreement No. 101022664

Elasticity modulus derived from geophysical field methods will differ from laboratory-obtained results due to the actual sample size that introduces scale effects.

Establishing a good understanding of the Dynamic elasticity modulus of the cap and reservoir before and after CO_2 injection is crucial to understanding how the rock formations involved will be affected over time. The stiffness of the rock is important as it affects how easily the CO_2 will flow through the reservoir and how it will permeate in the cap rock. In general, the stiffer the rock, the more difficult it is for fluids to flow through them. Less stiff rocks deform more easily in response to the applied force imposed by the fluid that tries to flow within the pores. The results presented in Tables 7.6 and 7.8 indicate the elasticity modulus for sedimentary rocks. Generally, the rocks are not as stiff as crystalline rock that are in the range of >100 GPa (Christaras et al., 1994).

All rock specimens were relatively weak when tested for tensile strength, with the lowest value of 0.8 Pa and higher 4.3 MPa. These values are typical for weathered mudstones and siltstones (Perras et al., 2014). However, the unweathered rocks in the subsurface will probably have a higher tensile strength.

In concludion the rocks may be ideal as rock caps due to low porosity and permeability, but fluid pressure within the rock should remain within specified limits; otherwise, the rock may easily fracture and result in CO_2 leakage or/and deform to allow the flow of CO_2.

Future work should include further sampling among different members of the formations to present statistical representativeness.

An important task of future and further work is to identify potential candidate members/beds of the Pentalofos and Eptachori formation that have suitable reservoir properties for CO_2 storage, i.e. porosity >10% and permeability > 100 mD.

The PilotSTRATEGY project has received funding from the European Union's Horizon 2020 research and innovation programme under grant agreement No. 101022664

7.4 References

M. Ciccotti, F. Mulargia, Differences between static and dynamic elastic moduli of a typical seismogenic rock, Geophysical Journal International, Volume 157, Issue 1, April 2004, Pages 474–477, https://doi.org/10.1111/j.1365-246X.2004.02213.x

Perras, M.A., Diederichs, M.S. A Review of the Tensile Strength of Rock: Concepts and Testing. Geotech Geol Eng 32, 525–546 (2014). https://doi.org/10.1007/s10706-014-9732-0

Christaras, B., Auger, F. & Mosse, E. Determination of the moduli of elasticity of rocks. Comparison of the ultrasonic velocity and mechanical resonance frequency methods with direct static methods. *Materials and Structures* 27, 222–228 (1994). https://doi.org/10.1007/BF02473036

References and formulas used in calculation.

Test	Correlation	Formula	Reference
Vp	C1 - Ed	$Ed = rn^2 * [(1+n)(1-2n)]/(1-n)$	BS 1881 Part 203: Recommendations for measurement of velocity of ultrasonic pulses in concrete.1986
Point Load	C1 - BTS	BTS = -0,023+(Is)/(0,968+0,076*Is)	2b - Effect of Freezing and Thawing on Physical and MechanRocks Properties of Sedimentary Rock. Autores: Safin Bahadin Hama Saeed, Younis M. Alshkane
	C2- BTS	BTS = Is/0,8	Concrete test
	C3 - BTS	BTS = 0,69*Is	2d) - Comment on ‘‘Point Load Test on Meta-Sedimentary Rocks and Correlation to UCS and BTS’’ by Diyuan Li and Lous Ngai Yuen Wong, Rock Mechanics and Rock Engineering,
	C4 - BTS	BTS = 0,9*Is	
	C5 - UCS	$UCS = 17,57*Is^{1,155}$	3 -(a e b) Hyam Saleh Daoud1, Kamal Ahmad Rashed2 &Younis M. Alshkane3 - Correlations of Uniaxial Compressive Strength andModulus of Elasticity with Point Load Strength Index, Pulse Velocity and Dry Density of Limestone andSandstone Rocks in Sulaimani Governorate, Kurdistan Region, Iraq., Journal of Zankoy Sulaimani
	C3 - E	$E = 11,409*Is^{0,9322}$	
Schmi	C1 - UCS	$UCS = 0,0004* R^{4,163}$	1 - Singgih Saptonoa, Suseno Kramadibratab, Budi Sulistiantob - "Using the Schmidt

The PilotSTRATEGY project has received funding from the European Union’s Horizon 2020 research and innovation programme under grant agreement No. 101022664

			Hammer on Rock Mass Characteristic in Sedimentary Rock at Tutupan Coal Mine " - International Symposium on Earth Science and Technology, CINEST 2012
	C2 - UCS	UCS = 2*R	1a - Singh et al. (1983) in Singgih Saptonoa, Suseno Kramadibratab, Budi Sulistiantob - "Using the Schmidt Hammer on Rock Mass Characteristic in Sedimentary Rock at Tutupan Coal Mine " - International Symposium on Earth Science and Technology, CINEST 2012
			2b - Singh et al. (1983) in Hyam Saleh Daoud1, Younis M. Alshkane 2 , Kamal Ahmad Rashed3 - Prediction of Uniaxial Compressive Strength and Modulus of Elasticity for Some Sedimentary Rocks in Kurdistan Region- Iraq using Schmidt Hammer. Kirkuk University Journal /Scientific Studies (KUJSS), Volume 13, Issue 1, March 2018, pp. (52-67) - ISSN 1992 – 0849
	C3 - UCS	UCS = 2,208*EXP0,067 *R	1b - Katz et al. (2000) in Singgih Saptonoa, Suseno Kramadibratab, Budi Sulistiantob - "Using the Schmidt Hammer on Rock Mass Characteristic in Sedimentary Rock at Tutupan Coal Mine " - International Symposium on Earth Science and Technology, CINEST 2012
	C4 - UCS	UCS = 4,85*R-76,18	2a - O´ Rourke (1989) in Hyam Saleh Daoud1, Younis M. Alshkane 2 , Kamal Ahmad Rashed3 - Prediction of Uniaxial Compressive Strength and Modulus of Elasticity for Some Sedimentary Rocks in Kurdistan Region- Iraq using Schmidt Hammer. Kirkuk University Journal /Scientific Studies (KUJSS), Volume 13, Issue 1, March 2018, pp. (52-67) - ISSN 1992 – 0849
	C1 - E	$E = 6,95*g^2*R-1,14*106*10^{-3}$	1c - Deere and Miller (1966) in Singgih Saptonoa, Suseno Kramadibratab, Budi Sulistiantob - "Using the Schmidt Hammer on Rock Mass Characteristic in Sedimentary Rock at Tutupan Coal Mine " - International

The PilotSTRATEGY project has received funding from the European Union's Horizon 2020 research and innovation programme under grant agreement No. 101022664

			Symposium on Earth Science and Technology, CINEST 2012
	C2 - E	$E = 0{,}0004*R^{3{,}2825}$	2 - Hyam Saleh Daoud1, Younis M. Alshkane 2, Kamal Ahmad Rashed3 - Prediction of Uniaxial Compressive Strength and Modulus of Elasticity for Some Sedimentary Rocks in Kurdistan Region- Iraq using Schmidt Hammer. Kirkuk University Journal /Scientific Studies (KUJSS), Volume 13, Issue 1, March 2018, pp. (52-67) - ISSN 1992 – 0849

The PilotSTRATEGY project has received funding from the European Union's Horizon 2020 research and innovation programme under grant agreement No. 101022664

8. Conclusions

1. Geomechanical data were successfully acquired for the 4 regions involved in this work package, which will be used in the later parts of PilotSTRATEGY, especially WP3 for the building of dynamic models.

2. For the Paris Basin (France), the measurement results are limited in number because there were few samples and because of very rigorous sample requirements. Elastic properties of the samples from the Charmottes well samples follow the carbonate goemechanical model of IFPEN, while the Vulaines samples have weaker mechanical properties for the measured porosity.

3. For the onshore Ebro Basin (Spain), a complete geomechanical characterization was carried out on the Torre de las Arcas section where good quality drilled samples were available, with additional field measurements on samples too soft to core. Significant differences in the mechanical response of rocks were found comparing materials of different sedimentary facies.

4. For the offshore Ebro basin, core samples suitable for analysis were not available. To overcome this, rock properties have been calculated using data from well logs using standard geophysical relationships for 3 wells. This work has obtained elastic parameters that are the best approximation with the data available to populate any future dynamic model in the area.

5. For the Lusitania Basin (Portugal), samples were taken from outcrops, the lack of samples collected at depths equivalent to the required depth for carbon storage is a constraint for the interpretation of the results. Laboratory measurement of the Point Load Strength Index Test was conducted with the determination of Uniaxial Compressive Strength using a Schmidt Hammer.

6. For the West Macedonia area (Greece), representative samples were collected at outcrops and tested for the required parameters. As with the Portugal samples, there is the question of how representative these are of the subsurface.

The PilotSTRATEGY project has received funding from the European Union's Horizon 2020 research and innovation programme under grant agreement No. 101022664

9. Appendix: experimental set-ups, measurement methodologies

9.1 Geomechanical measurements (IFPEN)

9.1.1 Ultrasonic measurements

The measurement of ultrasonic velocities is done using piezoelectric transducers placed on each side of samples: a pulse generator is used to generate waves on one side, and an oscilloscope is used to record and analyse the wave having passed through the sample (Figure 9-1). Before being recorded, the signal is amplified and averaged over 512 signals to improve signal-to-noise ratio.

The piezoelectric ceramics used in these transducers have a resonance frequency of 500 kHz: therefore, the measurements estimate the elastic moduli at 500 kHz. Two types of piezoelectric ceramics are used which make it possible to emit and receive compression waves (P-wave) or shear waves (S-wave). In our lab, piezo transducers are put in a support allowing them to apply a constant and reproductible force on sample.

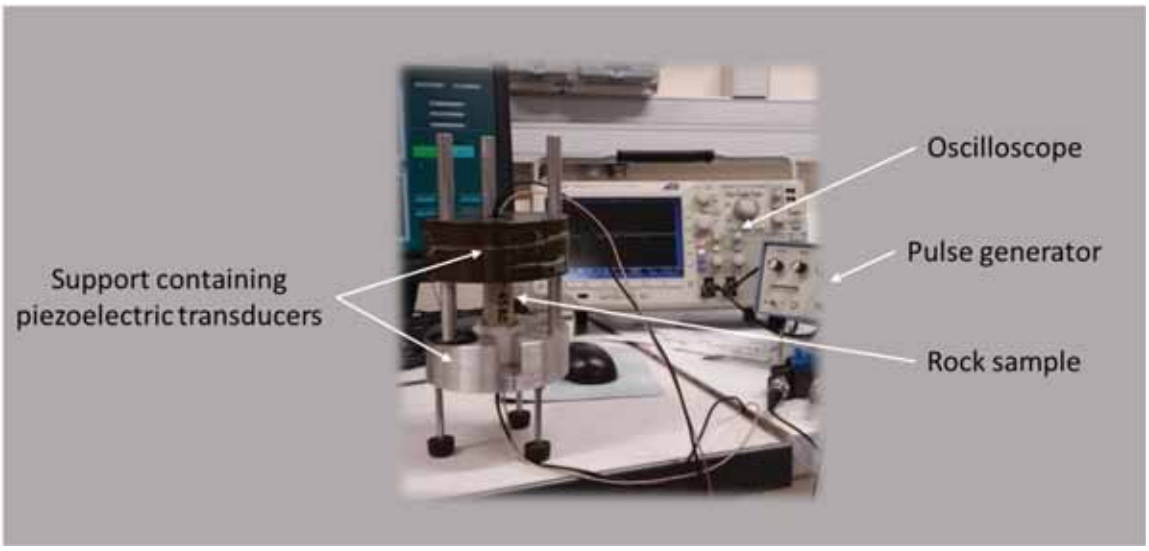

Figure 9-1: ultrasonic velocity measurement system

The measurement of the propagation times (with arrival time picking) of the two types of waves (P or S) allow to calculate the speed of the waves (V_P or V_S), which are linked to the elastic modulus by the following equations, in homogeneous assumption:

$$V_P = \sqrt{\frac{\lambda+2\mu}{\rho}} \text{ and } V_S = \sqrt{\frac{\mu}{\rho}},$$

where V_P and V_S are in m/s, λ and μ are Lamé coefficients in Pa, and μ is density in kg/m^3.

V_P and V_S can be expressed with other pairs of elastic parameters, using the Table 9-1.

Table 9-1: Relationship between isotropic elasticity parameters in 3D

(from https://fr.wikipedia.org/wiki/Module_d%27%C3%A9lasticit%C3%A9)

The PilotSTRATEGY project has received funding from the European Union's Horizon 2020 research and innovation programme under grant agreement No. 101022664

formules en 3D	(λ, G)	(E, G)	(K, λ)	(K, G)	(λ, ν)	(G, ν)	(E, ν)	(K, ν)	(K, E)	(M, G)
K [Pa] =	$\lambda + \frac{2G}{3}$	$\frac{EG}{3(3G-E)}$			$\frac{\lambda(1+\nu)}{3\nu}$	$\frac{2G(1+\nu)}{3(1-2\nu)}$	$\frac{E}{3(1-2\nu)}$			$M - \frac{4G}{3}$
E [Pa] =	$\frac{G(3\lambda+2G)}{\lambda+G}$		$\frac{9K(K-\lambda)}{3K-\lambda}$	$\frac{9KG}{3K+G}$	$\frac{\lambda(1+\nu)(1-2\nu)}{\nu}$	$2G(1+\nu)$		$3K(1-2\nu)$		$\frac{G(3M-4G)}{M-G}$
λ [Pa] =		$\frac{G(E-2G)}{3G-E}$		$K - \frac{2G}{3}$		$\frac{2G\nu}{1-2\nu}$	$\frac{E\nu}{(1+\nu)(1-2\nu)}$	$\frac{3K\nu}{1+\nu}$	$\frac{3K(3K-E)}{9K-E}$	$M - 2G$
G [Pa] =			$\frac{3(K-\lambda)}{2}$		$\frac{\lambda(1-2\nu)}{2\nu}$		$\frac{E}{2(1+\nu)}$	$\frac{3K(1-2\nu)}{2(1+\nu)}$	$\frac{3KE}{9K-E}$	
ν [1] =	$\frac{\lambda}{2(\lambda+G)}$	$\frac{E}{2G} - 1$	$\frac{\lambda}{3K-\lambda}$	$\frac{3K-2G}{2(3K+G)}$					$\frac{3K-E}{6K}$	$\frac{M-2G}{2M-2G}$
M [Pa] =	$\lambda + 2G$	$\frac{G(4G-E)}{3G-E}$	$3K - 2\lambda$	$K + \frac{4G}{3}$	$\frac{\lambda(1-\nu)}{\nu}$	$\frac{2G(1-\nu)}{1-2\nu}$	$\frac{E(1-\nu)}{(1+\nu)(1-2\nu)}$	$\frac{3K(1-\nu)}{1+\nu}$	$\frac{3K(3K+E)}{9K-E}$	

The analysis of the recorded signals can also be done by Fourier transform, to measure the phase velocity, by comparison with a known material.

Thus, ultrasonic measurements give 4 types of measurements, that can be performed on dry or satured samples:

- ${V_P}^i$ and ${V_S}^i$: P and S wave velocities measured with arrival time picking (i refers to impetus)
- ${V_P}^\varphi$ and ${V_S}^\varphi$: P and S wave velocities measured by Fourier transform (φ refers to phase).

9.1.2 Brazilian tests

The Brazilian test is one of the mechanical tests allowing to indirectly measure the breaking stress in uniaxial tension (UTS) on fragile materials. During the test, the cylindrical sample is placed horizontally between the platens of a press, and undergoes a compression, along two opposite generatrices (see Figure 9-2). To avoid heterogeneities in the loading, a cardboard is interposed between platens and sample: its thickness must be of few millimeters, and its width a must respect $\frac{a}{D} < 0.27$, to measure UCS with an error less than 10%). To have a valid test, the rupture must imperatively occur from the center, in the form of a single vertical fracture.

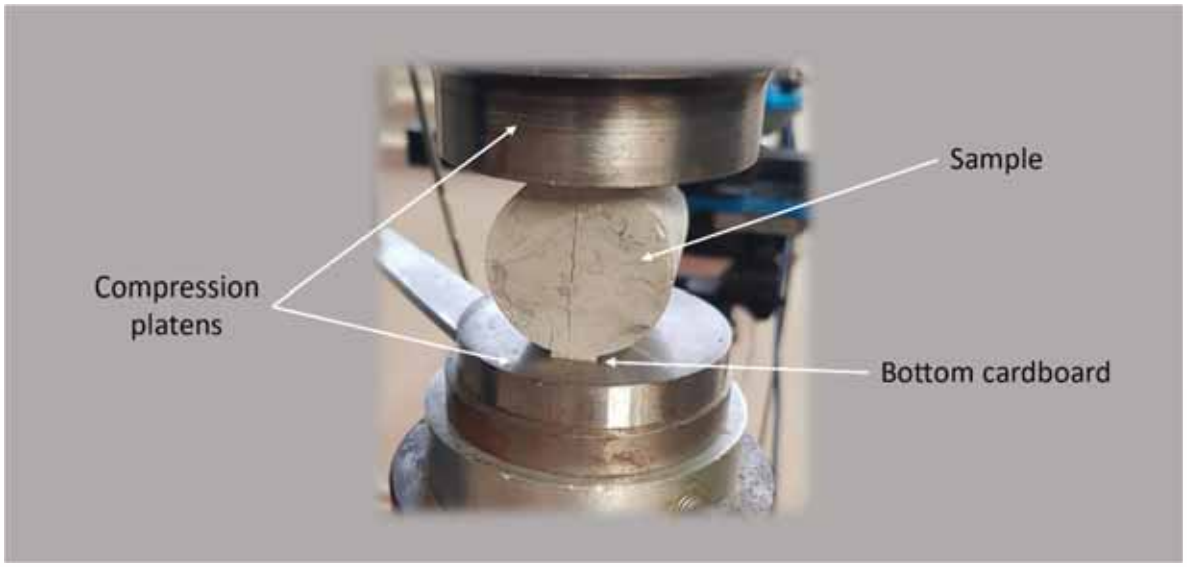

Figure 9-2: zoom on sample in Brazilian test condition

F being the breaking force, UTS is computed with the following equation

$$UTS = \frac{2F}{\pi DL}$$

9.1.3 Uniaxial compression tests

In this test, the cylindrical sample is placed vertically between the platens of a press, and undergoes a compression applied on the disc surface, along the axis of the specimen, which is unconfined (see Figure 9-3). Axial and lateral deformation must also be measured to derive elastic moduli and Poisson's ratio. Deformations can be measured by various device: due to small dimension of our samples (most of the samples had to be cut to respect the shapes required in this test), we choose to film the test to deduce the deformation by image correlation.

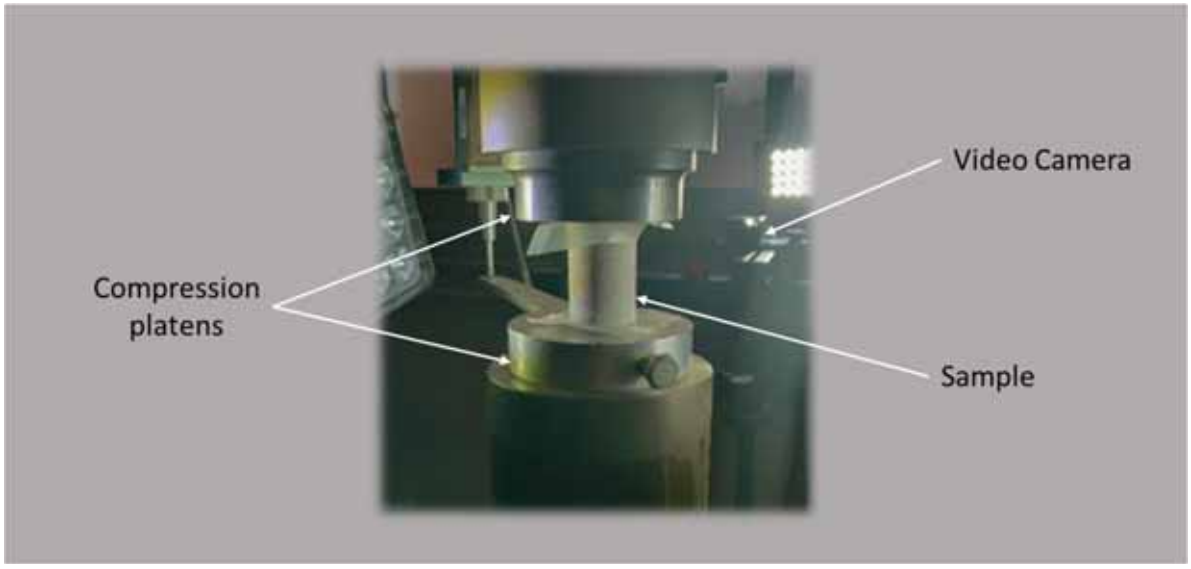

Figure 9-3: zoom on sample in uniaxial compression test condition

The PilotSTRATEGY project has received funding from the European Union's Horizon 2020 research and innovation programme under grant agreement No. 101022664

9.2 Geomechanical measurements (GALP)

Test	Parameters	Equation	Reference
Vp	Ed	$Ed = \rho * \vartheta^2 * \left[\frac{(1+\vartheta)*(1-2\vartheta)}{(1-\vartheta)}\right]$	BS 1881 Part 203:.1986
Point Load	BTS	$BTS = Is_{(50)} * 0.67$	Yagiz, S. (2013)
	UCS	$UCS = 17.57 * Is^{1.1555}$	Daoud et al. (2017)
	E	$E = 11.409 * Is^{0.9322}$	
Schmidt Hammer	UCS	$UCS = 2.208 * e^{0.067*R}$	Katz et al. (2000)
	E	$E = 6.95 * g^2 * R - 1.14 * 106 * 10^{-3}$	Deere and Miller (1966)

The PilotSTRATEGY project has received funding from the European Union's Horizon 2020 research and innovation programme under grant agreement No. 101022664

9.3 Refererences

Boulin P.F., Bretonnier P., Gland N., Lombard J.M. (2012), Contribution of steady state methods to water permeability measurement in very low permeability porous media, Oil Gas Sci. Technol. 67, 3, 387-401.

Egermann, P [P.], Lombard, J.-M., & Bretonnier, P. (2006). A fast and accurate method to measure threshold capillary pressure of caprocks under representative conditions. International Symposium of the Society of Core Analysts.

Dunn, K.-J., Bergman, D. J., & Latorraca, G. A. (2002). Nuclear magnetic resonance: Petrophysical and logging applications (1st ed.). Seismic exploration: v. 32. Pergamon.

Li S., Dong M., Li Z., Huang S., Qing H., Nickel E. (2005) Gas breakthrough pressure for hydrocarbon reservoir seal rocks: implications for the security of a long-term CO2 storage in the Weyburn field, Geofluids 5, 326-334.

The PilotSTRATEGY project has received funding from the European Union's Horizon 2020 research and innovation programme under grant agreement No. 101022664

10. ANNEXES

Studied samples in the three regions

10.1 Spain – Ebro Basin

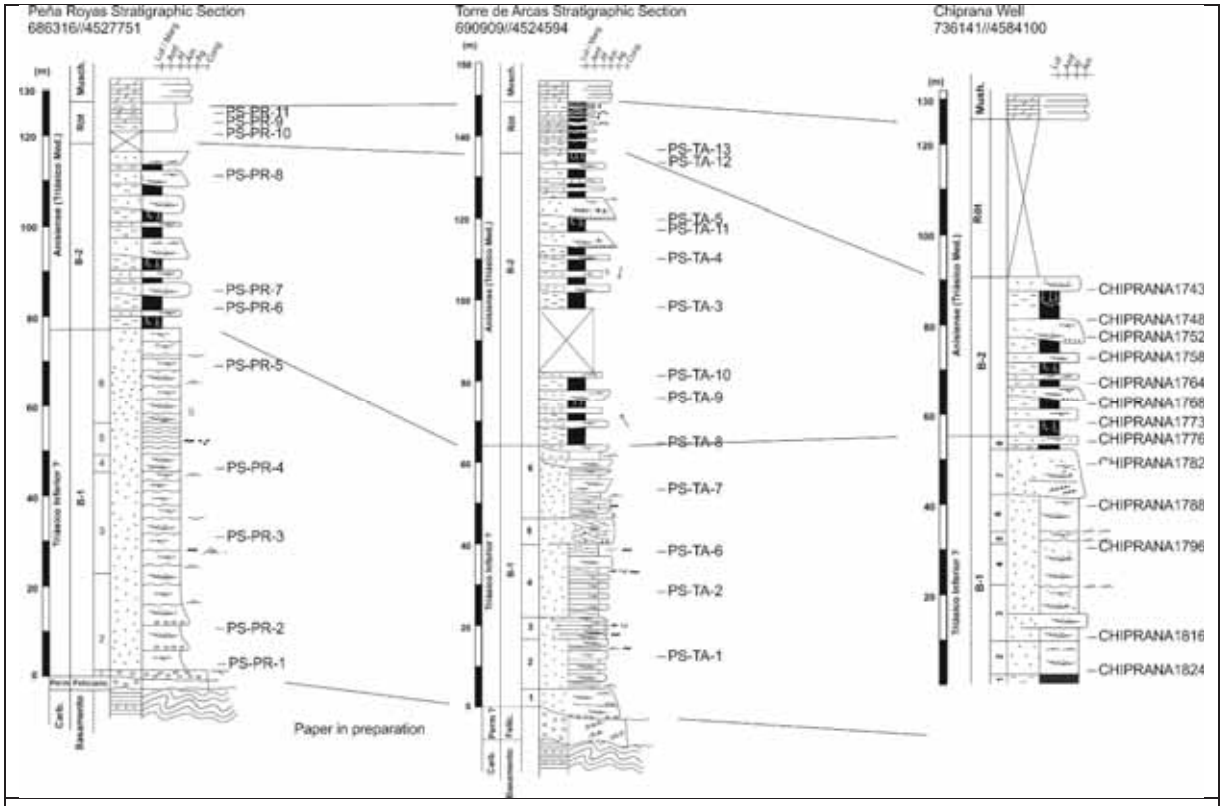

Localization of studied samples .

Samples of Peña Royas Section

The PilotSTRATEGY project has received funding from the European Union's Horizon 2020 research and innovation programme under grant agreement No. 101022664

Samples of Torre de Arcas Section

The PilotSTRATEGY project has received funding from the European Union's Horizon 2020 research and innovation programme under grant agreement No. 101022664

10.2 Portugal - Lusitanian Basin

Table – Studied samples from outcrops.

	**ARS-19** – Triassic Reservoir
	**ARS-20** – Triassic Reservoir

The PilotSTRATEGY project has received funding from the European Union's Horizon 2020 research and innovation programme under grant agreement No. 101022664

	**ARS-22** – Triassic Reservoir
	**CC-CV-4** – Triassic Reservoir

The PilotSTRATEGY project has received funding from the European Union's Horizon 2020 research and innovation programme under grant agreement No. 101022664

	**PRVT-23** – Triassic Seal
	**PPV-HT-28** – Triassic Seal

The PilotSTRATEGY project has received funding from the European Union's Horizon 2020 research and innovation programme under grant agreement No. 101022664

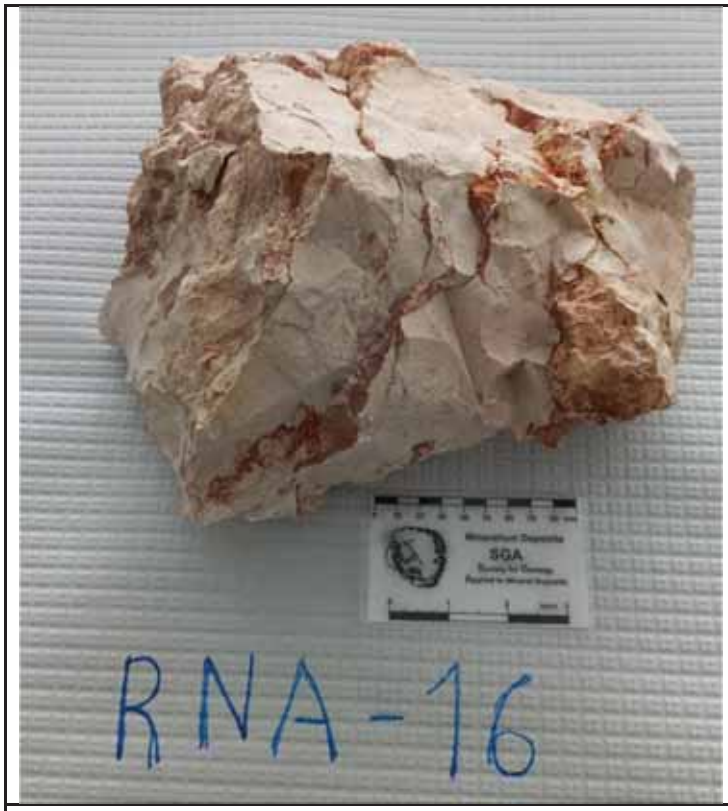	**RNA-16** – Cretaceous Seal
	**FR-SIB-26** – Cretaceous Seal

The PilotSTRATEGY project has received funding from the European Union's Horizon 2020 research and innovation programme under grant agreement No. 101022664

	**CD-DARN-14** - Cretaceous Reservoir
	**PAJ-29** – Upper Jurassic Reservoir

The PilotSTRATEGY project has received funding from the European Union's Horizon 2020 research and innovation programme under grant agreement No. 101022664

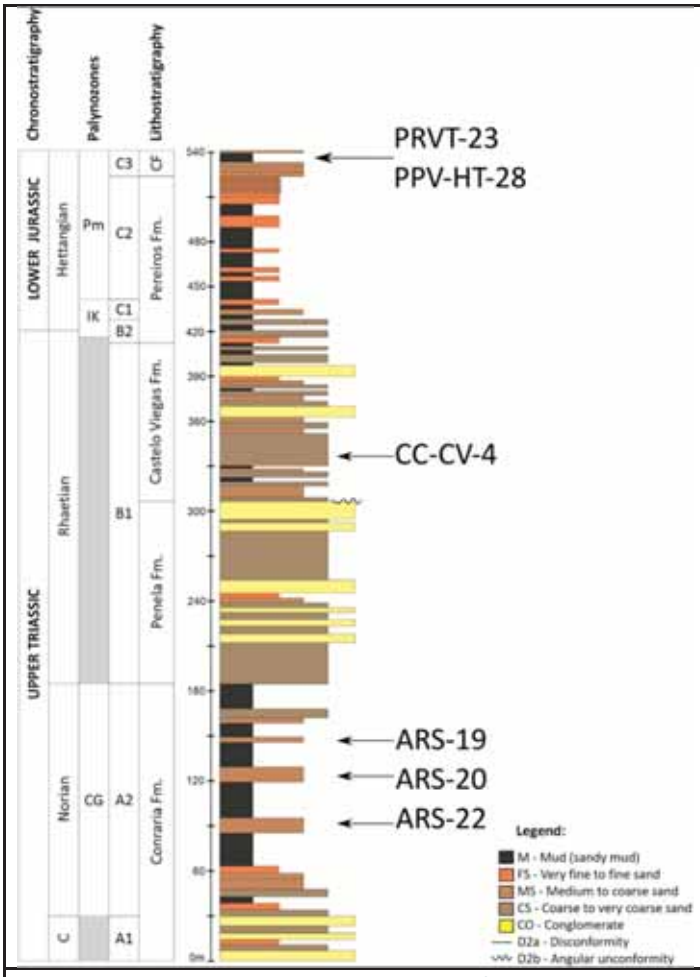

Figure … - Lithostratigraphic column of the Triassic storage complex, with location of the studied samples (adapted from Vilas-Boas et al., 2021).

The PilotSTRATEGY project has received funding from the European Union's Horizon 2020 research and innovation programme under grant agreement No. 101022664

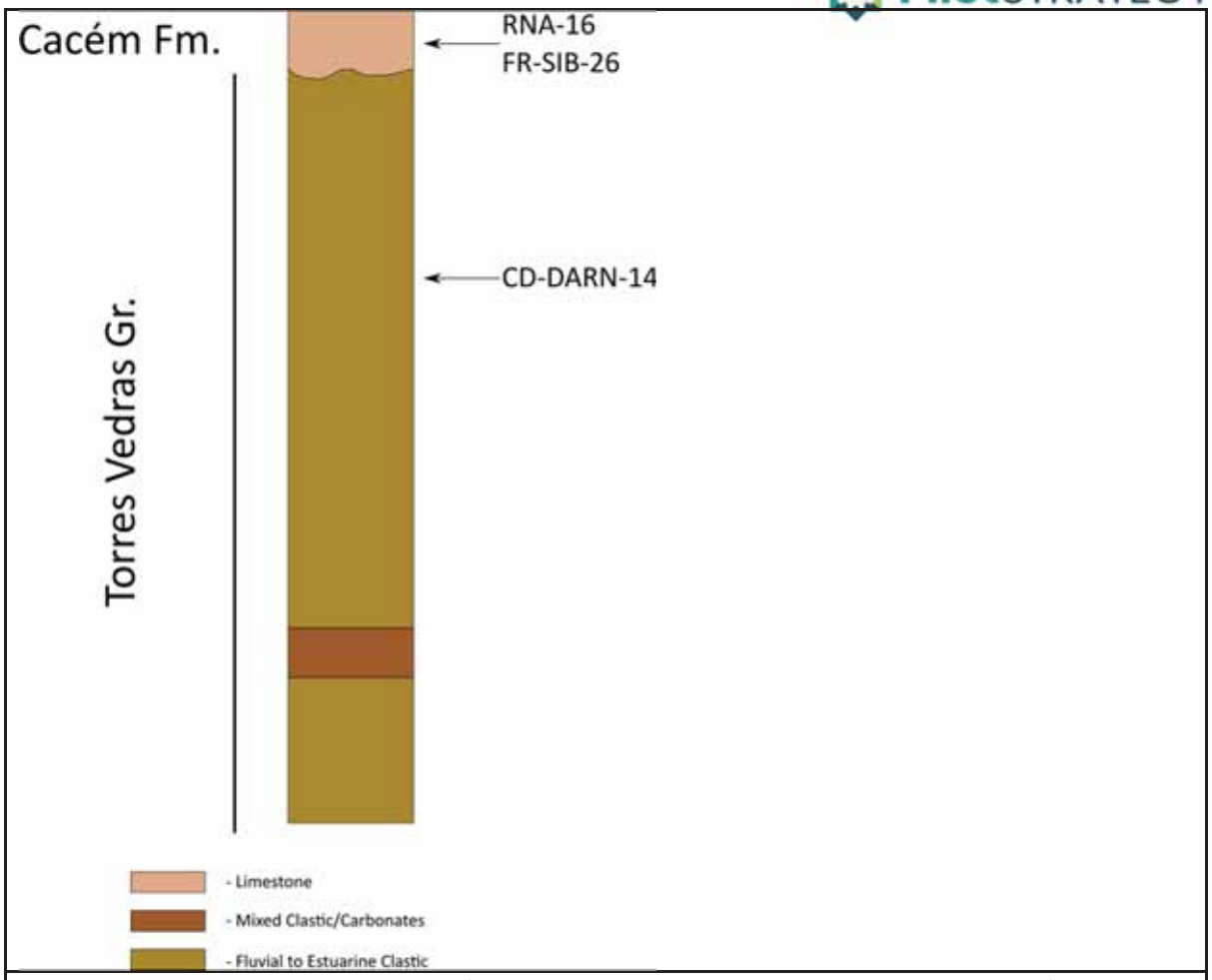

Figure … - Lithostratigraphic column of the Cretaceous storage complex, with location of the studied samples (adapted from Rey et al., 2006).

10.3 France - Paris Basin

Section / Well : CHARMOTTES-4

Autor(s) : BORDENAVE A.

Coordinates : Core K1 / K2
Top : 1790
Base : 1826

Scale 1/50

Sponge
Amygdaloid text.
Benthic forams.
Crinoids
Bryozoan
Bivalves
Pholadomya
Brachiopods
Pyrite
Echinid
Echin spines
Annelids
Gastropods
Corals
Corals clast
Marine bored surface
Bioturbations
Dolomitic concretions
Birdeyes
Pellets
Black gravels
Ooid
Oncoid

Texture: Mudstone, Wackestone, Packstone, Grainstone, Floatstone, Rudstone, Boundstone

Grain size: Clay, Silt, Fine sand, Medium sand, Coarse sand, Granule, Pebbles, Cobbles

Formation / Age | Core tray number | Core Number | Depth (m) | Lithology | Samples name | Core's photos and Samples selections | Sequential stratigraphy

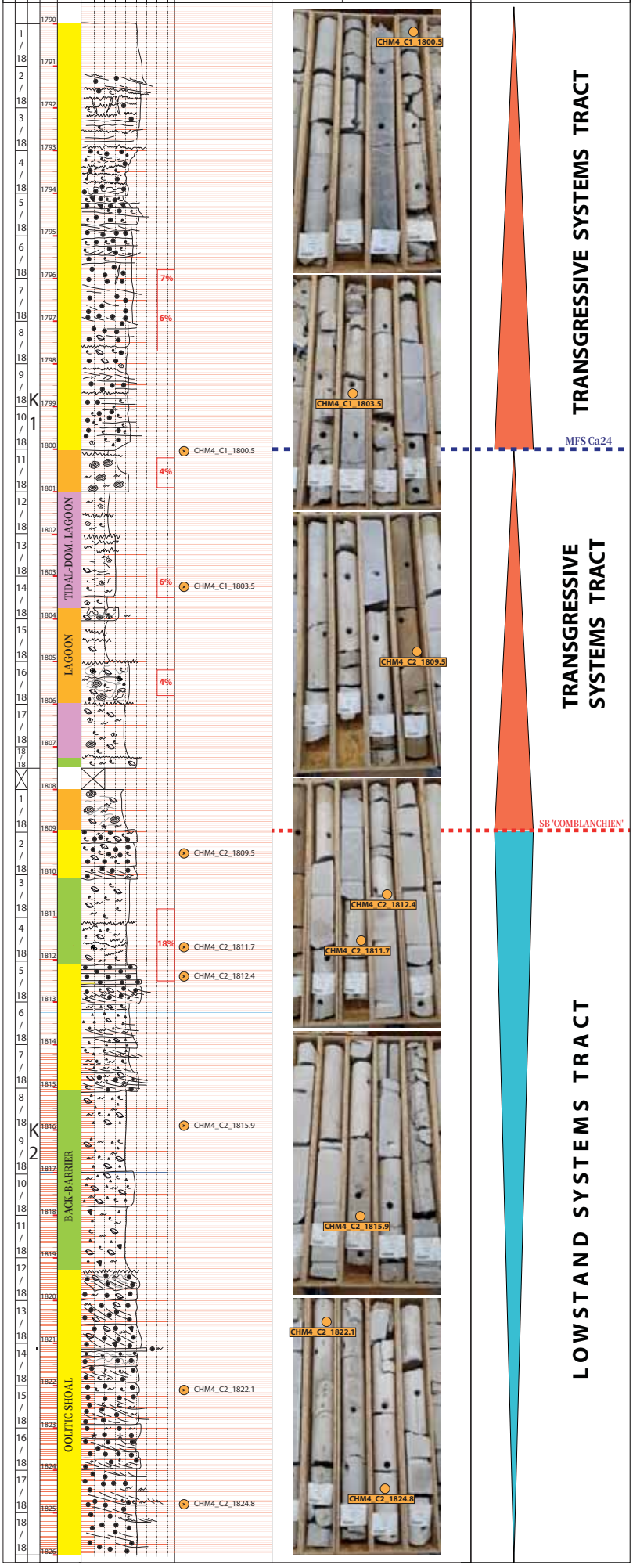

Section / Well : VULAINES-1

Auteur(s) : ISSAUTIER B.

Coordinates : Cores K6 / K7 / K8 / K9 / K10 / K11

Top : 1790
Base : 1820

Scale 1:50

Sponge
Amygdaloid text.
Benthic forams.
Crinoids
Bryozoan
Bivalves
Phabdotonya
Brachiopods
Pyrite
Echinid
Echin spines
Annelids
Gastropods
Corals
Corals clast
Marine bored surface
Bioturbations
Dolomitic concretions
Birdeyes
Pellets
Black gravels
Oncoid

Samples name

Core's photos and Samples selections

Sequential stratigraphy